


RESEARCH ARTICLE

Short- and long-term effects of perinatal phthalate exposures on metabolic pathways in the mouse liver

Kari Neier ¹, Luke Montrose¹, Kathleen Chen¹, Maureen A. Malloy¹, Tamara R. Jones¹, Laurie K. Svoboda¹, Craig Harris¹, Peter X.K. Song², Subramaniam Pennathur^{3,4}, Maureen A. Sartor^{2,5} and Dana C. Dolinoy^{1,6,*}

¹Environmental Health Sciences, University of Michigan, Ann Arbor, 1415 Washington Heights 48109 MI, USA; ²Biostatistics, University of Michigan, Ann Arbor, 1415 Washington Heights 48109 MI, USA; ³Division of Nephrology, Department of Internal Medicine, University of Michigan, Ann Arbor, 1500 East Medical Center Drive 48109 MI, USA; ⁴Department of Molecular and Integrative Physiology, University of Michigan, Ann Arbor, 1137 E. Catherine St. 48109 MI, USA; ⁵Computational Medicine and Bioinformatics, University of Michigan, Ann Arbor, 100 Washtenaw Avenue 48109 MI, USA and ⁶Nutritional Sciences, University of Michigan, Ann Arbor, 1415 Washington Heights 48109 MI, USA

*Correspondence address. NSF International Chair of Environmental Health Sciences, University of Michigan School of Public Health, 1415 Washington Heights, Ann Arbor, MI 48109, USA. Tel: +1-734-647-3155, Fax: 734-936-7283; E-mail: ddolinoy@umich.edu

Managing Editor: Toshi Shioda

Abstract

Phthalates have been demonstrated to interfere with metabolism, presumably by interacting with peroxisome proliferator-activated receptors (PPARs). However, mechanisms linking developmental phthalate exposures to long-term metabolic effects have not yet been elucidated. We investigated the hypothesis that developmental phthalate exposure has long-lasting impacts on PPAR target gene expression and DNA methylation to influence hepatic metabolic profiles across the life course. We utilized an established longitudinal mouse model of perinatal exposures to diethylhexyl phthalate and diisononyl phthalate, and a mixture of diethylhexyl phthalate+diisononyl phthalate. Exposure was through the diet and spanned from 2 weeks before mating until weaning at postnatal day 21 (PND21). Liver tissue was analyzed from the offspring of exposed and control mice at PND21 and in another cohort of exposed and control mice at 10 months of age. RNA-seq and pathway enrichment analyses indicated that acetyl-CoA metabolic processes were altered in diisononyl phthalate-exposed female livers at both PND21 and 10 months (FDR = 0.0018). Within the pathway, all 13 significant genes were potential PPAR target genes. Promoter DNA methylation was altered at three candidate genes, but persistent effects were only observed for *Fasn*. Targeted metabolomics indicated that phthalate-exposed females had decreased acetyl-CoA at PND21 and increased acetyl-CoA and acylcarnitines at 10 months. Together, our data suggested that perinatal phthalate exposures were associated with short- and long-term activation of PPAR target genes, which manifested as increased fatty acid production in early postnatal life and increased fatty acid oxidation in adulthood. This presents a novel molecular pathway linking developmental phthalate exposures and metabolic health outcomes.

Key words: endocrine disrupting chemicals; liver; metabolism; transcriptomics; metabolomics; DNA methylation

Received 19 July 2020; revised 9 September 2020; accepted 10 September 2020

© The Author(s) 2020. Published by Oxford University Press.

This is an Open Access article distributed under the terms of the Creative Commons Attribution Non-Commercial License (<http://creativecommons.org/licenses/by-nc/4.0/>), which permits non-commercial re-use, distribution, and reproduction in any medium, provided the original work is properly cited. For commercial re-use, please contact journals.permissions@oup.com

Introduction

Metabolic disorders, including obesity, diabetes, and non-alcoholic fatty liver disease, are increasing in prevalence and present a major concern for public health (1). Recently, exposures to environmental endocrine disrupting chemicals (EDCs), such as phthalates, have been suggested to interfere with metabolism to influence risk of metabolic disorders. Phthalates are found in a variety of consumer products, including plastics, furniture, and food packaging, resulting in ubiquitous exposure (2). Exposure to phthalates during early development has been linked to metabolic disruption, although the precise effects remain unclear. For example, some human birth cohort studies have reported that developmental exposure to phthalates resulted in increased body mass index and body fat percentage, while others have reported a lack of significant effect on body weight/composition (3–5). Insights into the molecular metabolic pathways that are perturbed by developmental phthalate exposures could provide clarity. Furthermore, the majority of animal studies that have examined metabolic effects of phthalates have focused on diethylhexyl phthalate (DEHP), despite the increasing risk for exposure to ‘newer’ phthalates that are understudied, such as diisononyl phthalate (DINP) (6). Inclusion of understudied phthalates, as well as phthalate mixtures, is needed to understand phthalate-associated metabolic health risks.

Several studies have indicated that phthalates interfere with metabolism by interacting with human and mouse peroxisome proliferator-activated receptors (PPARs) (7–11). PPARs are nuclear receptors that activate transcription of target genes regulating a wide variety of metabolic processes, including fatty acid biosynthesis, fatty acid oxidation, and glucose homeostasis (12–15). PPARs are present in rodents and humans in three main isoforms: PPAR α , PPAR γ , and PPAR δ/β . PPAR α expression is highest in the liver, PPAR γ expression is highest in adipose tissue, and PPAR δ/β is ubiquitously expressed across all tissues at low levels (16, 17). Phthalates have been demonstrated to interact with all three isoforms (7, 8, 10). During development, PPAR signaling is critical for programming of metabolic organs and tissues (18, 19). However, few studies have directly examined PPAR activation following developmental phthalate exposures (20, 21).

PPARs recruit ten-eleven translocation (TET) enzymes to the promoter regions of target genes to locally de-methylate DNA and facilitate transcription (22). DNA methylation is a well-established epigenetic modification that influences gene transcription and is heritable through cell division. DNA methylation consists of a methyl group bound to the 5' carbon of a cytosine (5mC), usually preceding an adjacent guanine (CpG). Higher levels of 5mC in the promoter region are associated with repression while lower levels of promoter 5mC are generally associated with activation (23). TET enzymes catalyze the oxidation of 5mC to 5'-hydroxymethylcytosine (5hmC), and then subsequently 5'-formylcytosine (5fC) and 5'-carboxylcytosine (5caC), which is removed by base excision repair machinery and replaced with an unmethylated cytosine (24). Contrary to 5mC, high levels of promoter 5hmC are associated with activated transcription (25, 26). During development, DNA methylation is particularly sensitive to environmental cues and undergoes reprogramming (27, 28). Specifically, TET enzymes catalyze the conversion of 5mC to 5hmC and facilitate epigenome-wide demethylation, followed by methylation by DNA methyltransferases (29). While DNA methylation is relatively stable and heritable through cell division, it is highly dynamic and responsive to the environment during development (30). Thus,

modification of DNA methylation by chemical exposures during development may result in altered DNA methylation that persists into adulthood.

For this study, we aimed to study developmental exposures of multiple phthalates that span both high-molecular weight (DEHP and DINP) and low-molecular weight (DBP) classes of phthalates that represent human exposure risk (6). DEHP and DBP have large bodies of toxicological and epidemiological literature, but health effects following DINP exposure are relatively under studied, despite increasing exposure risks as it began to replace DEHP in many products (6). We previously found that perinatal exposure to DEHP alone, DINP alone, and a combination of DEHP+DINP resulted in increased relative liver weights in weanling female mice at postnatal day 21 (PND21) (31), which may be indicative of PPAR α activation (32, 33). Longitudinally, female mice perinatally exposed to DEHP-only had increased body fat percentage and those perinatally exposed to DINP-only had impaired glucose tolerance (34). Building upon these findings, we hypothesized that early life exposures to phthalates resulted in long-lasting impacts on PPAR target gene expression in the liver by decreasing promoter region DNA methylation to influence metabolism across the life course. To investigate this hypothesis, we utilized liver tissue collected from a previously established mouse model of perinatal human-relevant exposures to DEHP-only, DINP-only, and DEHP+DINP. We used transcriptomics (RNA-seq) in liver collected in early postnatal life (PND21), immediately at the end of the exposure period, as well as at 10 months of age, long after the exposure had ceased, to screen for PPAR target genes that were persistently activated by developmental phthalate exposures. We then measured promoter region DNA methylation levels of candidate PPAR target genes to elucidate the role of DNA methylation. Finally, we investigated whether hepatic metabolic function was impacted by perinatal phthalate exposures via measurement of metabolites involved in central metabolism and fatty acid oxidation in the liver.

Materials and Methods

Animals and Exposures

The overall experimental design is laid out in Fig. 1 and is described in detail in previous studies (31, 34). Animals were obtained from a colony of viable yellow agouti (A^{vy}) mice, maintained for over 220 generations with sibling mating and forced heterozygosity for the A^{vy} allele through the male line (35). For this study, we utilized tissues from only the ‘wild-type’ a/a offspring, which are isogenic and 93% similar to C57BL/6 (36).

The exposure window captured the entire perinatal period spanning from pre-conception (2 weeks prior to mating) through gestation and lactation until weaning at PND21. Two weeks prior to mating, virgin a/a dams aged 6–8 weeks were randomly assigned to one of four exposure groups: (i) Control, (ii) DEHP-only, (iii) DINP-only, and (iv) DEHP+DINP. Phthalates (Sigma) were administered through the chow on a background 7% corn oil phytoestrogen-free diet (Teklad diet TD-95092; ENVIGO, Madison, WI). Controls were given 7% corn oil chow without phthalates added. Phthalates were mixed into corn oil from Envigo to create a stock solution, and the stock solution was sent back to Envigo where it was mixed with the corn oil used to produce custom 7% corn oil chow to achieve uniform distribution of phthalates within the chow. Exposure levels for the three exposure groups were as follows: DEHP-only = 25 mg DEHP/kg chow; DINP-only = 75 mg DINP/kg-chow; DEHP+DINP = 25 mg

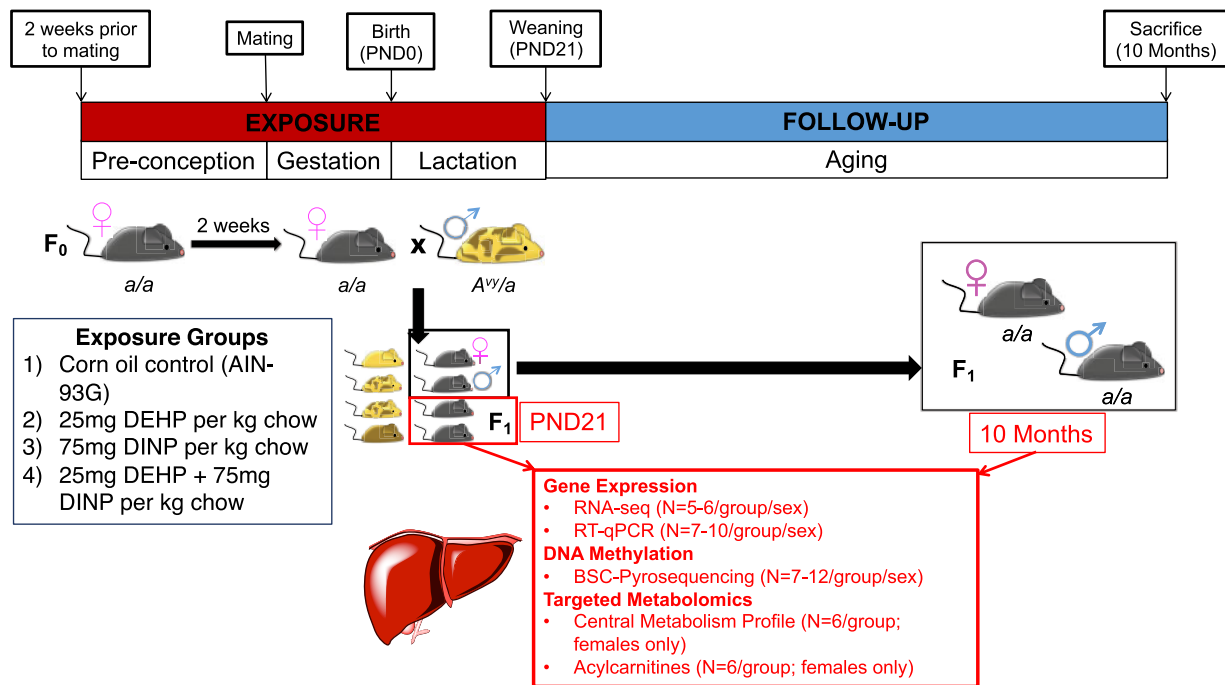


Figure 1: Experimental design. Two weeks prior to mating, virgin *a/a* female mice (F_0) were randomly assigned to one of four exposure groups containing different combinations of phthalates. Phthalates were administered through chow, on a background diet of 7% corn oil (phytoestrogen-free). Exposure spanned pre-conception, gestation, and lactation, and at weaning on PND21, one male and one female F_1 offspring per litter were weaned onto control chow and followed until 10 months of age. A cohort of mice were euthanized at PND21 and another were euthanized at 10 months of age, and livers were collected for analysis via RNA-seq, RT-qPCR, pyrosequencing of BSC DNA, and targeted metabolomics

DEHP + 75 mg DINP/kg chow. These exposure levels were selected based on a target maternal dose of 5 mg/kg-day for DEHP and 15 mg/kg-day for DINP, assuming that pregnant and nursing female mice weigh ~25 g and eat ~5 g of chow per day. These target doses were selected based on literature demonstrating obesity-related phenotypes in offspring that were developmentally exposed to 5 mg/kg-day of DEHP (37, 38). A higher exposure level of DINP was chosen based on previous studies that have indicated it is three times less potent than DEHP with respect to antiandrogenic effects (39). We assumed that relative potencies would be similar for metabolic effects since there are currently no potency estimates or animal literature for metabolic effects following developmental DINP exposure. The resulting exposure levels are estimated to fall within the range of exposures experienced by humans (31). This is based on amniotic fluid levels of phthalates found in humans (ranging from <LOD to 100.6 ng/ml) and a study in rodents that orally ingested 11 mg/kg-day of phthalates resulting amniotic fluid levels of 68 ng/ml (40–47). Since we used similar target doses of 5 and 15 mg/kg-day, we estimate that this results in similar amniotic fluid levels to 68 ng/ml which is within the range of human amniotic fluid levels.

At PND21, one male and one female *a/a* offspring per litter were weaned onto control chow and followed to 10 months of age while the rest of the *a/a* mice were euthanized at PND21 for tissue collection. Study mice that were followed to 10 months were co-housed with one same-sex, same-age, non-study littermate that was used as a companion only. Full litter parameters and outcomes are reported in previous work (31). There were no significant differences in number of pups per litter across exposure groups. Throughout the duration of the study, animals were given food and water ad libitum and remained on a 12-hour light/dark cycle. Health checks were carried out daily by

lab personnel and the University of Michigan Unit for Laboratory Animal Medicine. The guidelines for the use and care of laboratory animals were followed and mice were treated humanely. The University of Michigan Institutional Animal Care and Use Committee approved all animal procedures used for this project.

Tissue Collection and Nucleic Acid Isolation

At PND21, mice were fasted for 4 hours prior to euthanasia. At 10 months, mice were fasted for 6 hours prior to euthanasia. Estrus testing was performed on females at 10 months of age and synchronized so that all females were sacrificed during estrus. Euthanasia was carried out via inhalation of carbon dioxide (CO_2), followed by cardiac puncture exsanguination and whole-body perfusion with cell culture grade 0.9% sodium chloride saline (Sigma-Aldrich). Liver tissue was excised and weighed, then flash frozen in liquid nitrogen and stored at -80°C .

RNA and DNA were extracted from flash frozen livers of offspring aged PND21 and 10 months using Universal All-Prep kits (Qiagen Cat No. 80224). Approximately 10–15 mg of tissue from each liver was homogenized in lysis buffer using a TissueLyser II (Qiagen). Kit protocols were followed exactly. DNA and RNA quantity were measured using a NanoDrop2000 spectrophotometer. Isolated RNA and DNA were stored at -80°C .

RNA-seq Library Preparation and Sequencing

RNA-seq library preparation and sequencing were carried out at the University of Michigan Advanced Genomics Core in Ann Arbor, MI. RNA libraries from liver of PND21 and 10-month mice were sequenced (N = 5–6/sex/age). We excluded samples from mice that had gross liver tumors, then selected 5–6 samples for

each sex and each exposure group based on the highest RNA Integrity Numbers (RIN) as assessed by Agilent 2200 TapeStation analysis. Electropherograms indicated that the RINs ranged from 6.0 to 9.4 for RNA isolated from liver tissue. Library preparation for RNA isolated from liver was carried out using the Illumina TruSeq stranded mRNA Library Prep Kit following manufacturer instructions. Quantity and quality of the prepared libraries were confirmed with the Agilent 2200 TapeStation. Sequencing was carried out on the Illumina HiSeq 4000. Liver libraries were multiplexed across 8 sequencing lanes and were sequenced on one full flow cell to eliminate batch effects. Paired-end 50 bp reads were sequenced.

Bioinformatics Pipeline and Differential Expression

Sequenced reads were trimmed via Cutadapt (48), quality control assessed with FastQC (49), aligned using STAR (51), and expression quantification performed using RSEM (51), all with default parameters. The following quality parameters were assessed for each library: (i) number of unique reads, (ii) ratio of unique reads to duplicates, (iii) number of reads covering gene bodies, and (iv) area under the curve (AUC) for gene body reads. One liver sample had substantially lower reads (2.4 million unique reads and 2.1 million unique reads in gene bodies) than the others and was removed from downstream analyses. After removal of this sample, the number of unique reads ranged from 15.2 million to 74.4 million, the ratio of unique reads to duplicates ranged from 74.9% to 87.8%, the number of unique reads in gene bodies ranged from 12.5 million to 62.8 million, and the AUC for gene body reads ranged from 56.9% to 79.4%. Differential expression was analyzed using the quasi-likelihood function (QLF) of edgeR (52, 53) in R (www.r-project.org) between each exposure group compared to controls, stratified by age and sex. Genes with false discovery rates (FDRs) of < 0.10 were considered statistically significant. Another package in R, DESeq2 (54), was used to obtain normalized read counts for each gene for plotting purposes.

Pathway Analysis

Pathway enrichment analyses for Gene Ontology (GO) Biological Processes (BP) were carried out via RNA-Enrich using the LRpath website (55, 56). RNA-Enrich accounts and adjusts for potential bias in gene set enrichment testing due to increased statistical power to detect differential expression for genes that have larger read counts. In addition, RNA-Enrich utilizes information from all genes included in differential expression analyses and utilizes *P*-values to detect relevant gene pathways. Pathway enrichment analyses were also carried out using LISA (epigenetic Landscape *In Silico* deletion Analysis) from cistrome.org which leverages publicly available chromatin accessibility and Chromatin Immunoprecipitation Sequencing (ChIP-seq) data to identify transcriptional regulators of gene sets obtained from differential expression analyses (57). To perform a pathway analysis on differential gene expression from both PND21 and 10-month time points together, we applied Fisher's method (58) for data fusion on the *P*-values from PND21 and 10-month differential expression analyses. For example, we combined the *P*-values from differential expression between control females and DINP-only females at PND21 and *P*-values between control females and DINP-only females at 10 months. We utilized the mean reads of controls in RNA-Enrich and LISA.

RT-qPCR

Reverse transcription-quantitative PCR (RT-qPCR) was carried out for three candidate genes in liver collected from PND21 ($N = 7-10$ /group/sex) and 10-month mice ($N = 8-9$ /group/sex). RNA was converted to cDNA using iScript cDNA Synthesis Kits (Bio-Rad Cat No. 1708891) following manufacturer instructions. We utilized a reference gene panel (PrimePCR H384 Reference Gene Panels, Bio-Rad) to test for reference genes that were stable in liver tissue across exposure groups and sex using pooled samples with eight mice per pool. This was carried out for RNA collected from livers at PND21 and 30 reference genes in triplicate were analyzed using geNorm (59). The most stable genes based on geNorm *M* values were *Hmbs*, *Actb*, and *Psmc4* (Supplementary Fig. S1A). We also used geNorm to calculate *V* values, which is defined as systematic variation for repeated RT-qPCR experiments on the same gene and reflects the variation in the machine, enzymes, and pipetting. Our analyses indicated that using two reference genes would provide reliable results, with a geNorm *V* value of < 0.15 , and we therefore elected to use two reference genes: *Hmbs* and *Psmc4* (Supplementary Fig. S1B). We excluded samples from the analysis if melt curve data indicated poor sample integrity or if *C_q* values were larger than 38, which is indicative of very low copies of the mRNA being amplified, and therefore would be unreliable.

Quantitative PCR reactions were set up using PrimePCR assays for ATP-citrate lyase (*Acly*), citrate synthase (*Cs*), and fatty acid synthetase (*Fasn*) (Bio-Rad) and SsoAdvanced Universal SYBR Green Supermix (Bio-Rad) via the manufacturer's instructions. PrimePCR assays have been designed and experimentally validated to meet MIQE guidelines. Reactions were set up in 384-well plates so that all samples from PND21 mice were on one plate and all samples from 10-month mice were on a second plate. Samples were run in triplicate, and controls included a no template control, positive PCR control, and genomic DNA control. We analyzed one gene per plate using the CFX384 Real-Time PCR Detection System (Bio-Rad). The cycling protocol was as follows: (i) 2 minutes at 95°C × 1 cycle, (ii) 5 seconds at 95°C and 30 seconds at 60°C × 40 cycles, and (iii) melt curve with 0.5°C 5-second increments from 65 to 95°C. Relative expression was carried out via calculating delta *C_q*, comparing *C_q* values of each target gene to *C_q* values of the reference genes. The $2^{-\Delta\Delta C_q}$ method was used to estimate fold-change.

DNA Methylation

We measured DNA methylation using bisulfite conversion of DNA and subsequent PCR and pyrosequencing assays on liver from PND21 ($N = 7-12$ /group/sex) and 10-month mice ($N = 8-10$ /group/sex). We bisulfite converted (BSC) DNA isolated from liver tissue using Zymo EZ-96 DNA Methylation kits (Zymo Cat No. D5004) following manufacturer instructions, and then used targeted PCR and pyrosequencing to measure DNA methylation at individual CpGs in the promoter regions of three target genes: *Cs*, *Acly*, and *Fasn*. Supplementary Table S1 describes the pyrosequencing assay parameters, including chromosomal location, primer sequences, annealing temperatures, sequence to analyze, and amplicon length. Primers were designed using PyroMark Assay Design software 2.0 and the mm10 mouse genome. Pyrosequencing assays were designed to capture CpGs in the promoter regions of PPAR target genes. Publicly available data from Cistrome (cistrome.org) (60) was used to select regions that were adjacent to PPAR-binding sites

(Supplementary Fig. S2). DNA methylation levels were measured using the PyroMark Q96 ID instrument (Qiagen). All bisulfite-converted DNA from PND21 mice were run on one plate and samples from 10-month mice were run on another plate to reduce plate-to-plate batch effects. A subset of samples were run in duplicate to ensure that the coefficient of variation was <10% for each assay. Each PCR and pyrosequencing plate included BSC 0%, 25%, 50%, 75%, and 100% methylated DNA control reactions and a no template negative control reaction to ensure that the assay was functioning properly.

Targeted Metabolomics

Targeted metabolomics assays were carried out on a roughly 50 mg section of frozen liver tissue at the Molecular Phenotyping Core, Michigan Nutrition and Obesity Center. Two targeted assays were carried out: (i) a central metabolism profile and (ii) an acylcarnitine profile (61). The central metabolism assay included 61 analytes involved in multiple metabolic pathways, including the citric acid cycle (TCA cycle), glycolysis, and the pentose-phosphate shunt. Samples underwent solvent extraction and were subsequently separated on a 1 mm × 150 mm hydrophilic interaction liquid chromatography-specific column using a 35-minute cycle. Analytes were measured on a quadrupole time of flight mass spectrophotometer. The acylcarnitines assay was carried out to measure 30 acylcarnitine species subsequent to solvent extraction. The samples were separated via 20-minute RPLC cycle and measured on a liquid chromatography triple quadrupole mass spectrometer with multiple reaction monitoring methods. Both assays included internal standards. Measurements for all analytes were normalized to tissue weight and log-transformed prior to statistical analysis. Even-numbered C4–C20 acylcarnitines were summed as a read-out for fatty acid oxidation (62). A full list of analytes included in the central metabolism profile and acylcarnitine profile can be found in Supplementary Table S2.

Statistical Analyses

All statistical analyses were carried out using R version 3.5.2 (www.r-project.org, last accessed 9/29/20). All analyses were stratified by age and sex. Multiple ANOVA analyses were carried out to compare metabolites measured in the central metabolism profile with a Bonferroni correction factor applied to calculate FDRs; metabolites with FDRs < 0.10 were considered signals and evaluated with additional *post hoc* linear regression analyses comparing exposure groups to controls. Comparisons of relative expression as measured via RT-qPCR and DNA methylation levels were carried out via linear mixed effects models for PND21 mice and linear regression for 10-month mice comparing each exposure group to controls. Since a large portion of PND21 mice had littermates included in the RT-qPCR and DNA methylation studies, we used linear mixed effects models with litter-specific random effects to account for within-litter correlation. This was not an issue for 10-month mice because only one male and one female per litter were used and all analyses were stratified by sex. For the bisulfite-converted DNA methylation assay at CpGs in the promoter of Cs, there were several values of 0% methylation and therefore distributions were not normal. Therefore, we used generalized linear models with a zero inflation compound Poisson distribution available via the *cpim* package in R (63) to analyze differences between exposure groups and controls for data generated from this assay. A Bonferroni correction factor was applied to

RT-qPCR, DNA methylation, C4–C20 acylcarnitines, and *post hoc* targeted metabolomic analyses to account for multiple comparisons; three comparisons were made per analysis since there were three exposure groups and each were compared to the control group. For these analyses, we considered comparisons with adjusted P-values of < 0.05 as significantly different, and those < 0.10 to be marginally significant. Pearson correlation coefficients were used to examine relationships between relative expression as measured by RT-qPCR, DNA methylation, and metabolite levels in the liver.

Results

RNA-seq

To identify PPAR target genes that were persistently altered by perinatal phthalate exposures, we utilized transcriptomics via RNA-seq to screen for PPAR target genes and/or biologically-relevant metabolic pathways that were altered at an early-life time point when offspring were still directly exposed (PND21) and a later-life time point when offspring had not been exposed for several months (10 months; >9 months after exposure had ceased). Differential expression analyses comparing hepatic gene expression in exposed groups versus controls, stratified by age and sex, revealed that PND21 females perinatally exposed to DINP-only had the most differentially expressed genes (61 genes) with FDR < 0.10 (Table 1). PND21 females perinatally exposed to a combination of DEHP+DINP had one differentially expressed gene with FDR < 0.10, while PND21 females perinatally exposed to DEHP-alone did not have any with FDR < 0.10. Females at 10 months of age did not exhibit any differentially expressed genes at FDR < 0.10 by exposure group, nor did males at either PND21 or 10 months.

The top 10 differentially expressed genes in DINP female livers at PND21 are presented in Table 2, and the full list can be found in Supplementary Table S3. The top ten differentially expressed genes were *Atp2a1*, *Myh1*, *Fabp3*, *Tnni2*, *Acta1*, *Dsg1c*, *Pgam2*, *Ryr1*, *Clip4*, and *Tpm2*. A majority of the 61 differentially expressed genes were up-regulated; out of 61 differentially expressed genes (FDR < 0.10), 56 were up-regulated and only five were down-regulated (Fig. 2).

Pathway Enrichment Analysis

Since a primary objective of this study was to identify long-lasting alterations in gene expression in metabolic pathways influenced by perinatal phthalate exposures, we utilized pathway enrichment analyses to determine whether there were

Table 1: Differentially expressed genes in the livers of mice perinatally exposed to phthalates

	No. of Differentially expressed genes (FDR < 0.10)			
	PND21 females	10-month females	PND21 males	10-month males
DEHP vs. Control	0	0	0	0
DINP vs. Control	61	0	0	0
DEHP+DINP vs. Control	1	0	0	0

Differential gene expression was determined by the QLF in edgeR comparing each exposure group to controls. The number of differentially expressed genes in this table was determined by FDR < 0.10.

Table 2: Top 10 differentially expressed genes in PND21 DINP female livers versus controls

Gene symbol	LFC	P-value	FDR
<i>Atp2a1</i>	11.77168701	7.49E-06	0.038647
<i>Myh1</i>	11.30810269	8.60E-06	0.038647
<i>Fabp3</i>	11.58658065	1.68E-05	0.038647
<i>Tnni2</i>	10.72416927	1.69E-05	0.038647
<i>Acta1</i>	11.22848784	1.87E-05	0.038647
<i>Dsg1c</i>	-1.989642518	2.04E-05	0.038647
<i>Pgam2</i>	9.268813642	2.22E-05	0.038647
<i>Ryr1</i>	8.62230757	2.24E-05	0.038647
<i>Clp4</i>	7.161814544	2.50E-05	0.038647
<i>Tpm2</i>	4.626968688	2.67E-05	0.038647

Differential gene expression was determined by the QLF in edgeR comparing each exposure group to controls.

biologically relevant gene pathways that may have been impacted at both PND21 and 10 months. Although we did not observe differential gene expression by exposure at 10 months with $FDR < 0.10$, we considered the possibility that sets of biologically relevant genes may have been differentially expressed at relatively small effect sizes that were not detected via differential gene expression and $FDR < 0.10$. Thus, we utilized the RNA-Enrich function in LRpath to carry out gene set enrichment analysis for GO BP terms to examine BPs that may have been impacted by developmental phthalate exposures, and used LISA to examine transcriptional regulators that may be responsible for perturbation of hepatic gene expression by developmental phthalate exposures. To identify pathways and transcriptional regulators that were enriched at both PND21 and 10 months, we used Fisher's method to combine raw P -values from differential expression analyses for all measured genes at PND21 and at 10 months, and the resulting Fisher P -values were used as input for gene set enrichment.

Pathway analyses revealed several metabolic pathways in the liver that were potentially reprogrammed by perinatal phthalate exposures. The top 10 pathways for DEHP females, DINP females, and DEHP+DINP females are presented in Table 3; a list of the top ten enriched pathways in males is located in Supplementary Table S4. Females and males perinatally exposed to DINP had the largest number of enriched pathways at $FDR < 0.05$, with 12 and 15 pathways, respectively. Notable pathways that were enriched in PND21 and 10-month females perinatally exposed to DINP included acetyl-CoA metabolic process ($OR = 2.42$, $FDR = 0.0018$), acyl-CoA metabolic process ($OR = 2.10$, $FDR = 0.0018$), and thioester metabolic process ($OR = 2.10$, $FDR = 0.0018$), which are processes regulated by PPARs. DINP males also had several enriched metabolic pathways, including alpha-amino acid metabolic process ($OR = 2.49$, $FDR = 0.0006$), organic acid metabolic process ($OR = 1.69$, $FDR = 0.003$), dicarboxylic acid metabolic process ($OR = 2.50$, $FDR = 0.012$), and small molecule metabolic process ($OR = 1.50$, $FDR = 0.019$) (Supplementary Table S4).

Acetyl-CoA was the most significantly enriched hepatic pathway for DINP females. 13 genes drove enrichment of this pathway, all of which are potential PPAR target genes (Table 4), as indicated by PPARgene.org and cistrome.org by publicly available expression and ChIP-seq data, respectively. Of these 13 genes, 10 were up-regulated in DINP females compared to control females (unadjusted P -value ≤ 0.05) at either PND21 or 10 months: *Fasn*, *Acaca*, *Pdk4*, *Pdha1*, *Acacb*, *Acly*, *Acss2*, *Pdk2*, *Cs*,

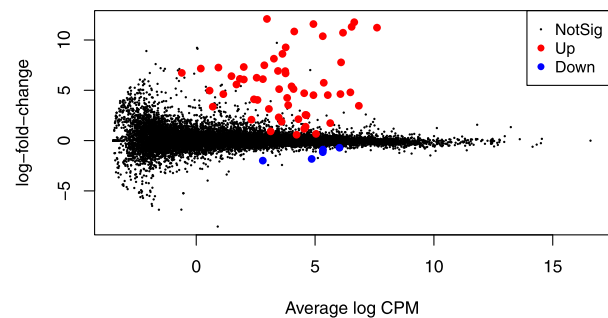
Differential Expression in PND21 DINP Females vs. Controls

Figure 2: Mean-difference plot of differential gene expression in PND21 DINP Females. Log-fold-change of gene expression for each gene (dots) in PND21-exposed females compared to PND21 control females is on the y axis, with average log CPM (counts per million reads mapped) on the x axis. Differentially expressed genes with $FDR < 0.10$ are colored red in genes that are up-regulated and blue in genes that are down-regulated in PND21 DINP females

and *Dlat*. Three of 13 genes were down-regulated in DINP females (unadjusted P -value ≤ 0.05) at either PND21 or 10 months: *Mpc1*, *Mlycd*, and *Mpc2*. Of the 10 up-regulated genes, four were up-regulated at both PND21 and 10 months (unadjusted $P \leq 0.05$ vs. controls): *Fasn*, *Pdk4*, *Acacb*, and *Cs* (Table 4). Out of the genes driving the acetyl-CoA metabolic process pathway, eight were potential PPAR α targets, 11 were potential PPAR γ targets, and five were potential PPAR δ/β targets. Notably, females perinatally exposed to DEHP-only and DEHP+DINP also exhibited differences in PPAR target gene expression, although these differences were less consistent than those observed in DINP-only females (Fig. 3A-L).

The most enriched pathway in males perinatally exposed to DINP across the PND21 and 10-month time points was alpha-amino acid metabolic process. Within this pathway, two of 15 significant genes were identified as potential PPAR target genes with experimental evidence, and another two were identified as potential PPAR target genes only due to putative PPAR response element (PPRE)-binding sites located flanking the transcription start site (TSS). However, in the second most enriched pathway in DINP males, organic acid metabolic process, 13 out of 33 significant genes in the pathway were identified as PPAR target genes with experimental evidence and two genes had PPREs flanking the TSS (Supplementary Table S5). Despite the relatively large number of PPAR target genes that were significant in this pathway, there was only one gene that had the same directional change to a degree of at least modest statistical significance (unadjusted $P < 0.10$) at both PND21 and 10 months: *Cyp2e1*. Furthermore, there was a mixture of up- and down-regulated genes at both PND21 and 10 months.

Since we hypothesized that developmental phthalate exposures exerted persistently altered changes in gene expression through activation of PPARs, we utilized LISA [cistrome.org (57)] as an unbiased approach to identify transcriptional regulators of genes perturbed by developmental phthalate exposures. The top transcriptional regulator of PND21 and 10-month DINP females was *RXR α* ($P = 5.89 \text{ E-}24$; Supplementary Table S6), the obligate heterodimer partner of PPARs. Further supporting a role of PPARs in developmental DINP exposure, PPAR α and PPAR γ were also both identified as potential transcriptional regulators in DINP females ($P = 8.07 \text{ E-}22$ and $2.2 \text{ E-}17$, respectively; Supplementary Table S6). In addition, CEBPA and CEBPB were top hit transcriptional regulators in DINP females ($P = 4.05 \text{ E-}23$, $P = 1.8 \text{ E-}22$, respectively), and are critical hepatic transcription

Table 3: Top 10 enriched GO BPs pathways across PND21 and 10-month female livers

Pathway	DINP				DEHP+DINP				
	No. of genes	Odds ratio	P-value	FDR	Pathway	No. of genes	Odds ratio	P-value	FDR
Epithelial cell apoptotic process	27	3.444	3.46E-05	0.21	Acetyl-CoA metabolic process	35	2.417	6.02E-07	0.001
Vascular endothelial growth factor signaling pathway	7	6.741	6.81E-05	0.21	Acyl-CoA metabolic process	60	2.103	8.76E-07	0.001
Positive regulation of phospho-protein phosphatase activity	4	8.227	1.65E-04	0.25	Thioester metabolic process	60	2.103	8.76E-07	0.001
Protein K63-linked deubiquitination	5	6.848	2.10E-04	0.25	Skeletal muscle contraction	5	5.258	3.79E-06	0.005
Hepatocyte apoptotic process	6	6.039	2.47E-04	0.25	Myofibril assembly	10	2.924	7.19E-06	0.008
Positive regulation of protein dephosphorylation	10	4.629	2.47E-04	0.25	Muscle contraction	46	2.041	8.08E-06	0.008
Purine nucleobase metabolic process	12	5.793	3.94E-04	0.32	Multicellular organismal movement	8	3.192	1.96E-05	0.015
Response to organic substance	737	1.475	4.21E-04	0.32	Musculo-skeletal movement	8	3.192	1.96E-05	0.015
Response to chemical	1000	1.423	5.09E-04	0.34	Monocarboxylic acid biosynthetic process	106	1.719	4.11E-05	0.028
Positive regulation of phosphatase activity	5	6.136	6.45E-04	0.37	Thioester biosynthetic process	22	2.372	6.77E-05	0.036
					Steroid metabolic process	188	2.337	1.74E-04	0.091

Pathway analyses were carried out via the RNA-Enrich function in LRpath for GO BPs. A combination of P-values from differential expression analysis at PND21 and 10 months calculated via Fisher's method was used for input into LRpath. Pathways above are enriched and do not include depleted pathways. Pathways were considered significantly enriched with FDR < 0.05.

factors that also occupy many of the same binding sites as PPARs in the liver (64). PPAR α , PPAR γ , RXR α , CEBPA, and CEBPB were also implicated as transcriptional regulators in DEHP and DEHP+DINP females (all $P < 0.05$), though to a lesser extent (Supplementary Table S6). Transcriptional regulators identified in the livers of males perinatally exposed to phthalates exhibited similar patterns to those seen in females. PPAR α , RXR α , CEBPA, and CEBPB were all also within the top 10 transcriptional regulators of genes perturbed in PND21 and 10-month males perinatally exposed to DINP ($P < 1.21 \text{ E}-8$), and PPAR γ was also a potential transcriptional regulator ($P = 6.13 \text{ E}-6$, Supplementary Table S6). These transcription factors were also potential transcriptional regulators of genes perturbed in males perinatally exposed to DEHP and DEHP+DINP, but to a lesser extent (Supplementary Table S6).

RT-qPCR

We next carried out RT-qPCR to examine relative expression for three genes that are involved in acetyl-CoA metabolic processes and were identified as being altered in the liver by perinatal exposure to phthalates in females: *Acly*, *Cs*, and *Fasn*. Analyses of RT-qPCR for relative expression of these three genes were confirmatory of the RNA-seq expression patterns at PND21. Females perinatally exposed to DINP-only and DEHP+DINP had increased relative expression of *Cs* (adjusted $P = 0.033$ and 0.040 , respectively) (Fig. 4A). Females perinatally exposed to DEHP+DINP also had increased relative expression of *Acly* and *Fasn* in the liver at PND21 (adjusted $P = 0.015$ and 0.007 , respectively) (Figs 3E and 4C). Females perinatally exposed to DINP-only also showed increased *Fasn* expression relative to controls at a degree nearing statistical significance (adjusted $P = 0.081$) (Fig. 4C). Although there was not a statistically significant difference in hepatic expression of *Acly* at PND21 via RNA-seq reads, the trends in *Acly* expression at PND21 across exposure groups was similar between RNA-seq (Fig. 3C) and RT-qPCR data (Fig. 4C).

In livers collected from females at 10 months, RT-qPCR relative expression data were less consistent with RNA-seq expression data than they were for PND21 livers. In contrast to RNA-seq results, there were no statistically significant differences in relative expression of *Cs* or *Fasn* at 10 months via RT-qPCR (adjusted $P > 0.10$; Fig. 4B and F). Relative hepatic *Acly* expression, however, was increased in 10-month females perinatally exposed to DINP-only (adjusted $P = 0.012$), and was increased to a degree nearing statistical significance in DEHP+DINP females compared to controls (adjusted $P = 0.097$) (Fig. 4D). RNA-seq data indicated similar trends in hepatic *Acly* expression across exposure groups (Fig. 3D).

RT-qPCR assays for *Acly*, *Fasn*, and *Cs* were also carried out in livers collected from males at PND21 and 10 months. Males perinatally exposed to DINP had decreased relative expression of *Cs* in the liver at 10 months (adjusted $P = 0.028$). However, there were no other statistically significant relationships between relative hepatic expression of *Fasn*, *Acly*, or *Cs* and perinatal exposures to phthalates at PND21 or 10 months of age in males.

DNA Methylation

Since PPARs can recruit TET enzymes to de-methylate promoter region DNA of PPAR target genes (22), we measured CpG methylation levels in the promoter regions of *Acly*, *Fasn*, and *Cs* in the livers collected from mice at PND21 and 10 months of age. To do this, we utilized bisulfite conversion of DNA coupled with PCR and pyrosequencing. Pyrosequencing assays were designed

Table 4: Significant genes driving pathway enrichment for acetyl-CoA metabolic process in DINP females

Gene	PPAR target gene based on expression	PPAR target gene based on ChIP-seq	No. of PPREs in TSS-flanking region	No. of ChIP-seq peaks	PND21 LFC	PND21 P-value	10-month LFC	10-month P-value
Fasn	PPARα, PPARδ/β	PPARα, PPARγ	5	17	1.62	0.011*	1.66	0.0074**
Acaca	NA	PPAR γ	NA	16	0.76	0.06 [^]	1.53	0.0041**
Pdk4	PPARα, PPARδ/β, PPARγ	PPARα, PPARα	2	31	2.49	0.0011**	1	0.053*
Pdha1	PPAR α	PPAR α	0	4	0.54	0.015*	0.16	0.32
Acacb	PPARα, PPARγ	PPARγ	6	24	1.49	0.014*	1.39	0.0015**
Acly	PPAR δ/β	PPAR α , PPAR γ	6	3	0.76	0.17	1.44	0.0091**
Mpc1	NA	PPAR δ , PPAR β	NA	5	-0.48	0.015*	-0.47	0.13
Acss2	PPAR δ/β , PPAR γ	PPAR γ	8	1	1.24	0.08 [^]	1.31	0.027*
Mlycd	PPAR α , PPAR δ/β , PPAR γ	PPAR α , PPAR γ	2	9	-0.25	0.13	-0.45	0.0085**
Pdk2	PPAR γ	NA	9	NA	0.11	0.55	0.75	0.005**
Cs	PPARγ	PPARγ	3	5	0.76	0.0016**	0.58	0.0099**
Mpc2	NA	PPAR α , PPAR γ	NA	6	-0.26	0.29	-0.9	0.01**
Dlat	PPAR α , PPAR γ	NA	3	0	0.3	0.099 [^]	0.55	0.0054**

Genes were identified as PPAR target genes based on PPARgene.org, which utilizes a combination of evidence from published datasets and PPREs in regions flanking the TSS, and cistrome.org, which utilizes ChIP-seq data to identify transcription factor-binding sites in the promoter region. PND21 and 10-month log LFC and P-values (unadjusted) are from differential gene expression of RNA-seq data analyzed via edgeR QLF comparing DINP females to controls. Bolded genes were differentially expressed with an unadjusted P-value of ≤ 0.05 at both PND21 and 10 months.

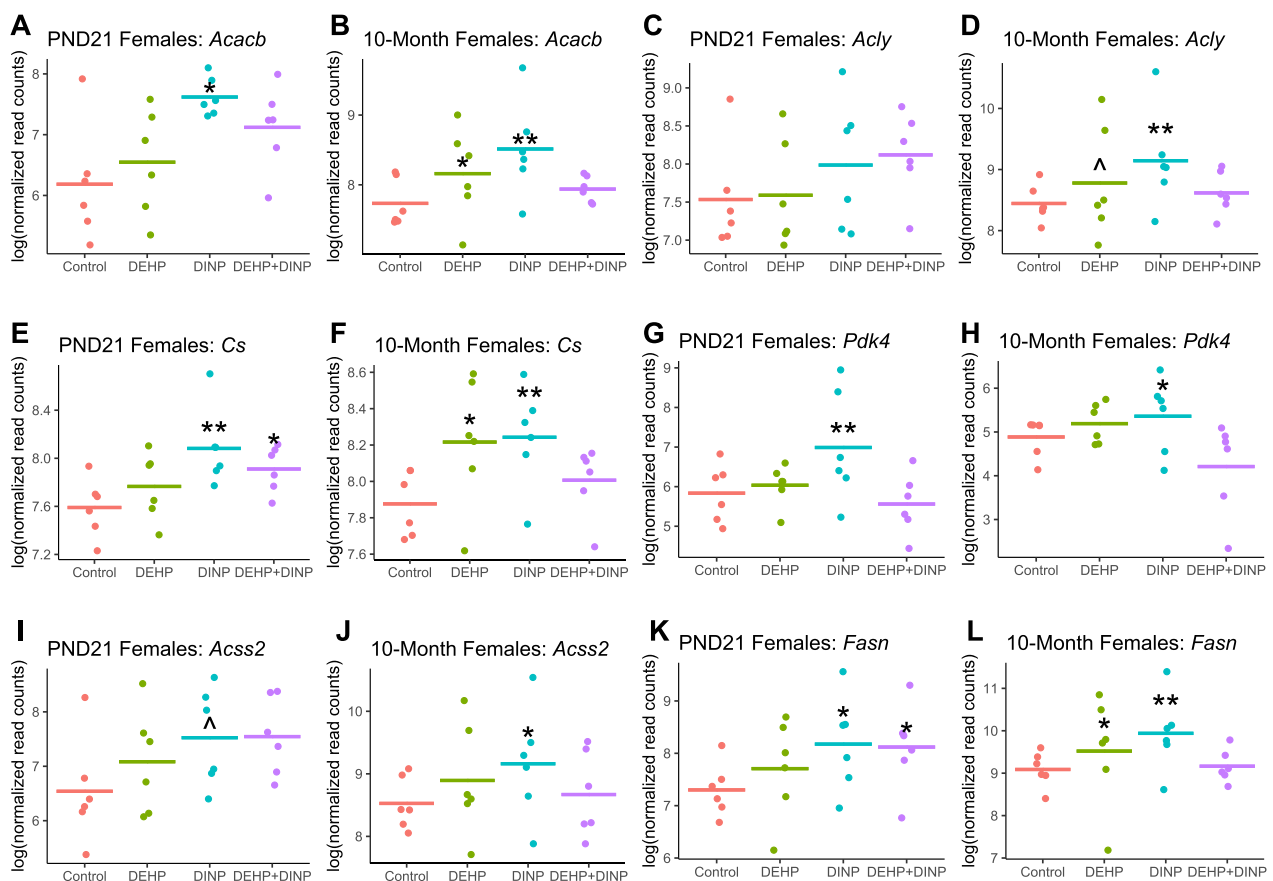


Figure 3: RNA-seq read counts for select PPAR target genes in the acetyl-CoA metabolic process pathway. Read counts for each gene were normalized to library size and log transformed for data visualization. (A) PND21 females: *Acacb*, (B) 10-month females: *Acacb*, (C) PND21 females: *Acly*, (D) 10-month females: *Acly*, (E) PND21 females: *Cs*, (F) 10-month females: *Cs*, (G) PND21 females: *Pdk4*, (H) 10-month females: *Pdk4*, (I) PND21 females: *Acss2*, (J) 10-month females: *Acss2*, (K) PND21 females: *Fasn*, (L) 10-month females: *Fasn*. All symbols represent unadjusted P-values from differential expression analyses in edgeR comparing each exposure group to controls. [^]P < 0.10, *P < 0.05, **P < 0.01. N = 5–6/group/age

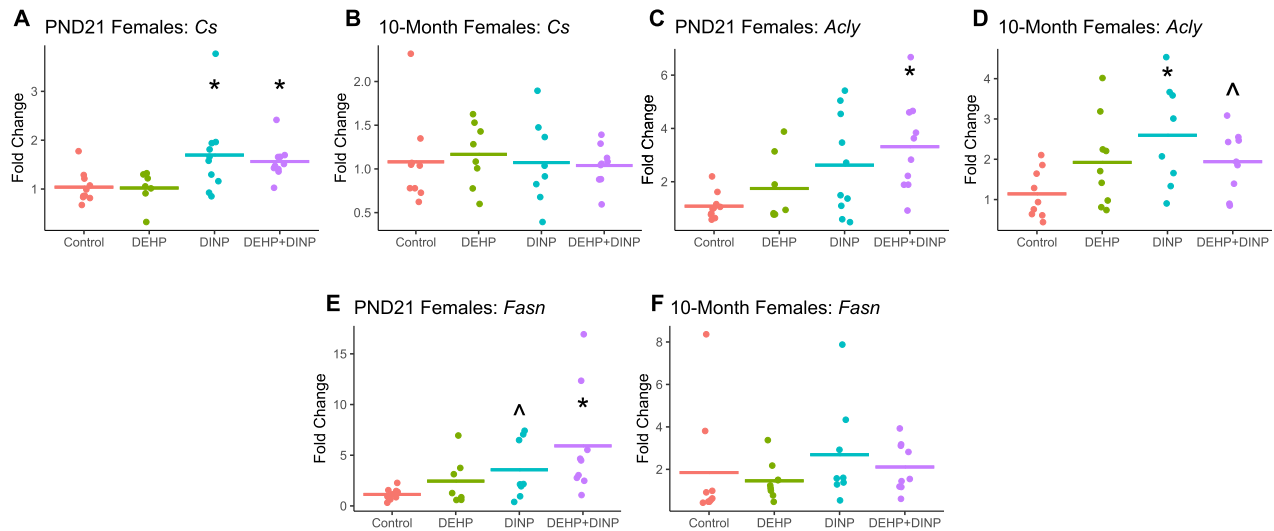


Figure 4: RT-qPCR for candidate PPAR target genes in the liver. Fold change was calculated via the 2^{-ddCq} method and plotted for data visualization. (A) PND21 females: Cs, (B) 10-month females: Cs, (C) PND21 females: *Acly*, (D) 10-month females: *Acly*, (E) PND21 females: *Fasn*, (F) 10-month females: *Fasn*. Relative expression [$Cq_{target} - \text{mean}(Cq_{reference})$] was compared for each exposure group to controls using 1) linear mixed effects models with litter as the random effect in analyses on PND21 mice, 2) and linear regression in analyses on 10-month mice. P-values were Bonferroni corrected for multiple comparisons. ^ $P < 0.10$, * $P < 0.05$. $N = 7-10/\text{group/age}$

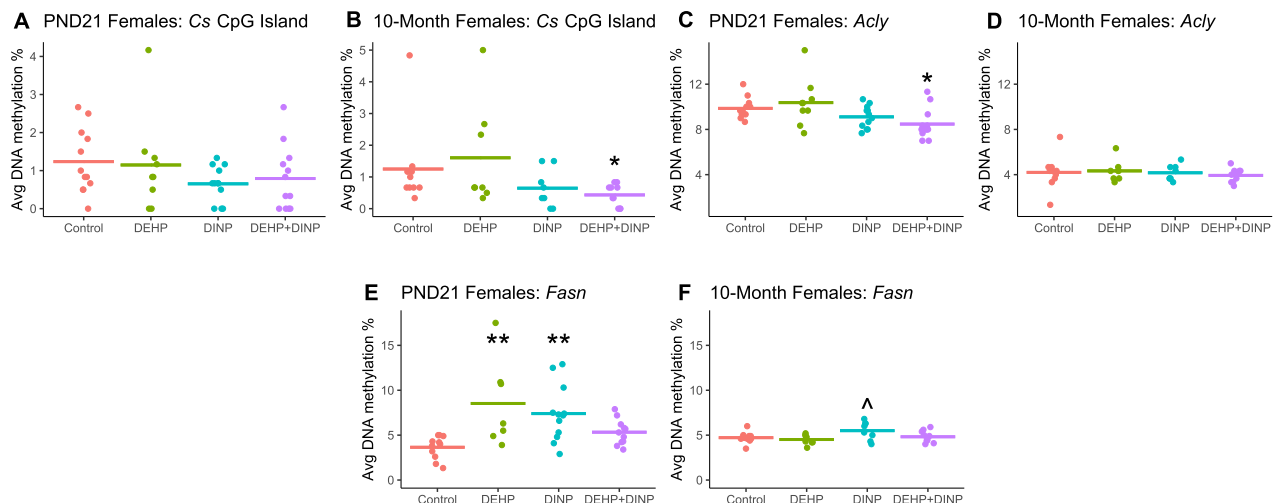


Figure 5: Promoter DNA methylation in candidate PPAR target genes. (A) PND21 females: Cs, (B) 10-month females: Cs, (C) PND21 females: *Acly*, (D) 10-month females: *Acly*, (E) PND21 females: *Fasn*, (F) 10-month females: *Fasn*. Mean DNA methylation across CpG sites was compared for each exposure group to controls using 1) linear mixed effects models with litter as the random effect in analyses on PND21 mice, 2) linear regression in analyses on 10-month mice, and 3) compound Poisson regression with zero inflation in analyses of Cs DNA methylation. P-values were Bonferroni corrected for multiple comparisons. ^ $P < 0.10$, ** $P < 0.05$. $N = 7-12/\text{group/age}$

to capture CpG-rich regions adjacent to PPAR-binding sites in the promoter regions of the three genes (Supplementary Fig. S2). PPAR ChIP-seq peaks from Cistrome (cistrome.org) (60) were used to visually identify potential PPAR α - and PPAR γ -binding sites on the genome.

Females perinatally exposed to phthalates had altered DNA methylation levels in the promoter regions of *Cs*, *Acly*, and *Fasn* (Fig. 5). At PND21, there were no statistically significant differences in *Cs* promoter region DNA methylation levels in females between control and exposure groups, although non-statistically significant trends were reflective of mRNA expression level patterns across exposure groups (Figs 3E, 4A and 5A). Hepatic DNA methylation in the *Cs* promoter was 1.06% lower in 10-month females perinatally

exposed to DEHP+DINP compared to controls (adjusted $P = 0.04$) (Fig. 5B). As noted above, hepatic *Cs* expression was increased in females perinatally exposed to DEHP+DINP at PND21, but not at 10 months of age.

In PND21 females, promoter *Acly* DNA methylation percentages in the liver reflect *Acly* expression levels at PND21 (Figs 3C, 4C and 5C). Compared to control females, females perinatally exposed to DEHP+DINP had a 1.39% decrease in percent DNA methylation in the *Acly* promoter region at PND21 (adjusted $P = 0.048$). This was in concordance with RT-qPCR expression data which indicated that DEHP+DINP females had increased hepatic *Acly* expression at PND21. Despite our observations that there were changes in hepatic mRNA expression of *Acly* in females perinatally exposed to DINP-only and DEHP+DINP

relative to controls at 10 months of age, there were no statistically significant exposure-related changes in *Acly* promoter region DNA methylation at 10 months (Fig. 5D).

Fasn promoter region DNA methylation levels were unexpectedly increased in livers from female mice perinatally exposed to phthalates at PND21 and 10 months of age when compared to controls (Fig. 5E and F, respectively). At PND21, females perinatally exposed to DEHP-only and DINP-only had higher percent methylation than control females by 4.88% and 3.75%, respectively (adjusted $P=0.002$ and 0.007 , respectively). This was the largest effect size observed for DNA methylation in this study. Females perinatally exposed to DINP-only also had modestly increased hepatic DNA methylation in the *Fasn* promoter compared to controls (effect size = 0.78%; adjusted $P=0.084$). Interestingly, the observed increase in *Fasn* promoter region DNA methylation in DINP-only females corresponded to increased *Fasn* expression at both time points, which was unanticipated based on typical relationships between promoter region DNA methylation and gene expression.

Males perinatally exposed to phthalates exhibited minimal effects on hepatic DNA methylation in the promoter regions of *Cs*, *Acly*, and *Fasn* (Supplementary Fig. S3). The only statistically significant difference was in males perinatally exposed to DEHP+DINP at PND21, who had increased DNA methylation in the CpG island of the *Cs* promoter compared to controls (effect size = 0.91%, adjusted $P=0.013$). However, there was no complementary significant alteration in *Cs* expression in DEHP+DINP males at PND21.

Hepatic Central Metabolism Profile

To determine whether perinatal phthalate and phthalate mixture exposures impacted central metabolism in the liver, we utilized a targeted metabolomic assay to profile metabolites involved in the TCA cycle. Metabolites were measured only in the livers collected from females, since phthalate-related alterations in hepatic gene expression and DNA methylation were observed primarily in females.

Female mice perinatally exposed to phthalates exhibited an altered hepatic acetyl-CoA metabolism profile at both PND21 and 10 months. At PND21, ANOVA tests for central metabolism metabolites indicated that acetyl-CoA levels differed across exposure groups (FDR=0.054). No other metabolites exhibited exposure-related statistically significant differences at PND21 based on an ANOVA FDR < 0.10, and there were no metabolites that had an ANOVA FDR < 0.10 in 10-month livers. Post hoc analyses were carried out for both PND21 and 10-month livers on acetyl-CoA to examine differences between each exposure group and controls and to investigate whether changes at PND21 persisted to 10 months (Fig. 6). Hepatic acetyl-CoA levels were decreased in PND21 females perinatally exposed to DEHP+DINP compared to controls (adjusted $P=0.0005$; Fig. 6A). In contrast, at 10 months of age, acetyl-CoA levels were higher in DEHP+DINP females compared to control females (adjusted $P=0.013$; Fig. 6B). In addition, 10-month-old females perinatally exposed to DINP-only also had increased hepatic acetyl-CoA relative to controls to a marginal degree of statistical significance (adjusted $P=0.068$; Fig. 6B). Results from ANOVA analyses for the full list of measured metabolites are available in Supplementary Tables S7 and S8.

In addition to being associated with perinatal phthalate exposures, hepatic acetyl-CoA levels were also associated with gene expression and promoter DNA methylation in livers from PND21 females. Increased relative expression (as measured by

RT-qPCR) and decreased promoter DNA methylation of *Acly* were associated with decreased acetyl-CoA levels ($P=0.006$ for both; adjusted $R^2=0.35$ and 0.26 , respectively; Fig. 6C and D). Increased *Fasn* gene expression in PND21 livers was also associated with decreased acetyl-CoA levels ($P=0.017$, adjusted $R^2=0.28$), but DNA methylation in the *Fasn* promoter was not correlated with acetyl-CoA ($P=0.26$; adjusted $R^2=0.02$). Neither *Cs* gene expression nor promoter methylation demonstrated a relationship with acetyl-CoA levels in PND21 livers. Despite hepatic acetyl-CoA's association with perinatal phthalate exposures at 10 months of age, it was not associated with expression or promoter DNA methylation of *Acly*, *Fasn*, or *Cs*.

Hepatic Acylcarnitine Profile

Acylcarnitines were profiled in the liver using a targeted metabolomic approach since elevated even-numbered C4–C20 acylcarnitine levels can be indicative of incomplete fatty acid oxidation and have been linked to insulin resistance in human studies (62). As with hepatic central metabolism metabolite measures, acylcarnitines were profiled only in female livers.

At 10 months of age, females perinatally exposed to phthalates showed signs of incomplete fatty acid oxidation in the liver. This was evidenced by increased hepatic C4–C20 acylcarnitine levels in the DEHP-only, DINP-only, and DEHP+DINP compared to controls (adjusted $P=0.011$, 0.033 , and 0.061 , respectively; Fig. 7B). However, there were no significant differences in hepatic acylcarnitine levels between exposed and control mice at PND21 (Fig. 7A). Furthermore, neither gene expression nor promoter DNA methylation of *Acly*, *Fasn*, and *Cs* demonstrated a significant relationship with hepatic acylcarnitines at PND21 ($P > 0.10$).

Discussion

The findings presented here are consistent with previous studies that have demonstrated phthalates' abilities to activate PPAR α , PPAR γ and PPAR δ/β (7, 8, 10), and provide additional evidence that PPAR-regulated pathways may be impacted both in the short- and long-term in the liver (Fig. 8). We found that expression of genes perturbed by developmental phthalate exposures included genes regulated by PPAR α and PPAR γ , as well as the obligate heterodimer RXR α and related transcription factors CEBPA and CEBPB. Our data indicated that acetyl-CoA metabolism was altered in the liver of female mice perinatally exposed to DINP and a mixture of DEHP+DINP, with differential effects by age/time since exposure and phthalate. At PND21, hepatic acetyl-CoA levels were significantly decreased in females exposed to DEHP+DINP, but at 10 months, they were increased in females exposed to DINP-only and DEHP+DINP. Hepatic acylcarnitines were elevated in females from all three exposure groups relative to controls, but only at 10 months of age. DINP-only PND21 females exhibited the most alterations in hepatic gene expression, including PPAR target genes.

Pathway enrichment analyses of RNA-seq data in the liver indicated that metabolic pathways regulated by PPAR α , PPAR γ and PPAR δ/β were altered in DINP-only female livers at PND21 and 10 months of age, indicating that these pathways were potentially reprogrammed by perinatal exposure to DINP. Utilizing RNA-Enrich allowed us to examine perturbations in biological pathways cumulated from low-level changes in gene expression of groups of genes within these pathways. The genes that were drivers of the top enriched biological pathway, acetyl-CoA metabolic process, are likely PPAR target genes (Fig. 9). These genes

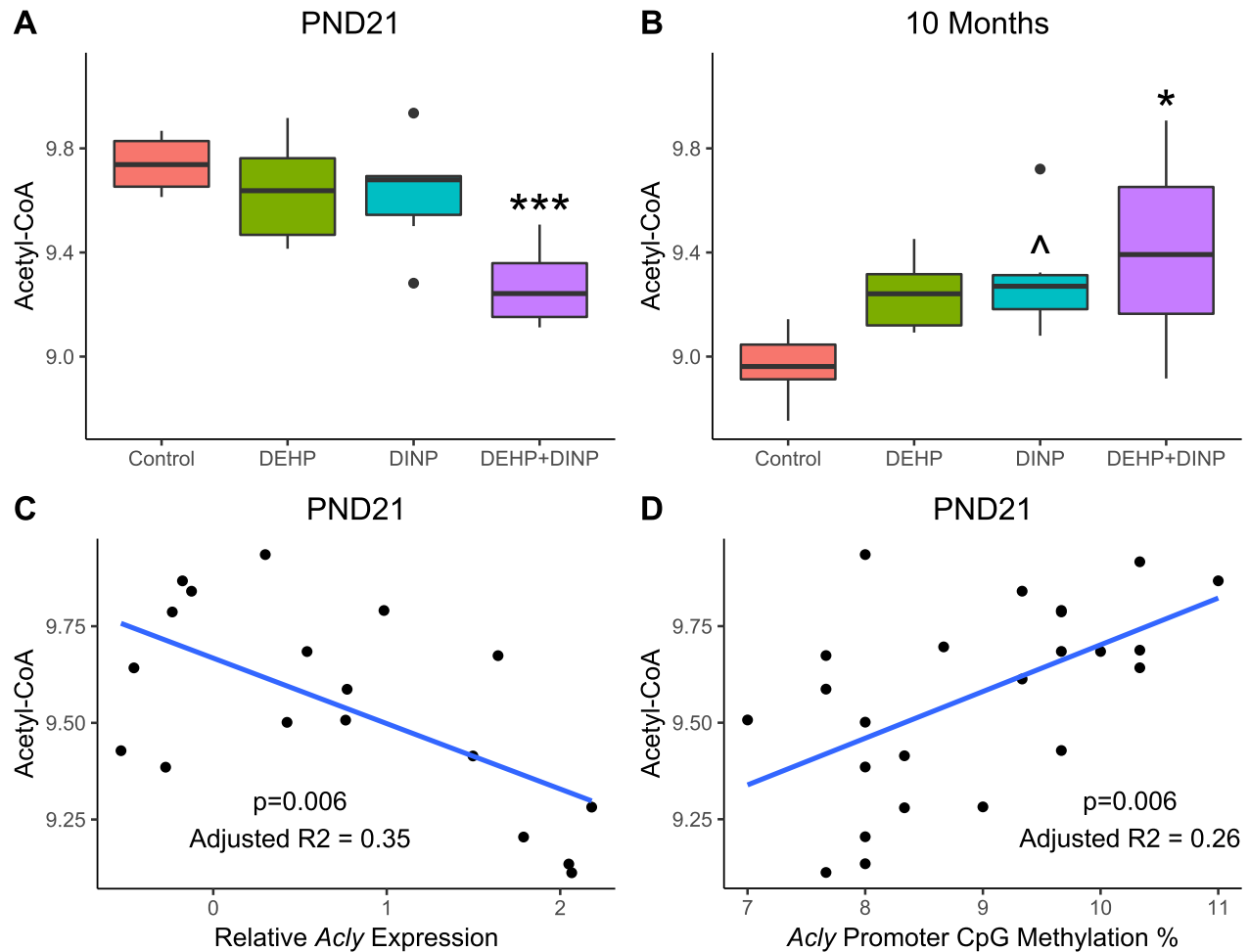


Figure 6: Hepatic acetyl-CoA levels and their relationship with *Acly* mRNA expression and DNA methylation. Differences in hepatic acetyl-CoA levels between exposure groups and the control group in females at (A) PND21 ($N=6$ /group) and (B) 10 months ($N=6$ /group). Associations between hepatic acetyl-CoA levels and (C) *Acly* mRNA expression as measured via RT-qPCR ($N=4-6$ /group) and (D) DNA methylation at 3 CpG sites in the *Acly* promoter ($N=6$ /group) in PND21 females. In boxplots, the boxes represent the interquartile range (IQR) and lines extend to 1.5*IQR, while dots are observations outside 1.5*IQR. In the dot plots, dots represent individual observations and blue lines are the best fit linear regression line. Post hoc comparisons of acetyl-CoA levels between exposure groups and the control group were evaluated with multiple linear regression of log-transformed data with the control as the reference group. Corrections for multiple comparisons were made using a Bonferroni correction factor. Associations between log-transformed acetyl-CoA levels and *Acly* expression and methylation were made using Pearson's correlation. $^{\wedge}P < 0.10$, $^*P < 0.05$, $^{***}P < 0.001$ versus the control group

were predominantly up-regulated and some genes showed increased expression levels in the DEHP-only and DEHP+DINP exposure groups as well. Taken in context with the observed age-specific alterations in hepatic acetyl-CoA and acylcarnitine levels, our data indicate that developmental phthalate exposures interfere with acetyl-CoA metabolism and fatty acid metabolism both in early postnatal life immediately following exposure, and in adulthood long after exposure had ceased (Fig. 9). However, the specific effects on these pathways differed by age. For example, *Acly* and *Fasn* expression were inversely associated with acetyl-CoA levels only in PND21 livers, suggesting that lower levels of acetyl-CoA in phthalate-exposed PND21 females may have been due to increased fatty acid production (Fig. 9). However, the increased acetyl-CoA observed in DINP and DEHP+DINP females at 10 months of age may have been due to increased fatty acid oxidation. Even-numbered C4–C20 acylcarnitines were elevated in livers from females perinatally exposed to phthalates compared to controls, suggesting up-regulation of the fatty acid oxidation pathway (62). Further supporting this,

post hoc examination of hepatic *Cpt1b* expression patterns in transcriptomic data indicated that it was up-regulated in all three phthalate-exposed groups compared to controls at 10 months of age with a log fold-change difference of between 1.48 and 1.76 (DEHP-only $P=0.01$, DINP-only $P=0.0031$, DEHP+DINP $P=0.0094$; Supplementary Fig. S4). Taken together, our findings suggest that at PND21, the response to perinatal phthalate exposures was increased fatty acid synthesis, whereas at 10 months, the response was increased fatty acid oxidation.

Despite the relatively few previous studies that have examined hepatic gene expression changes following developmental phthalate exposures, our findings were generally consistent with studies that have examined developmental exposures to other chemicals that interfere with metabolism and in studies that evaluated direct exposures to DEHP and other PPAR agonists. In concordance with our data, mice that were directly exposed to 200 or 1150 mg/kg-day of DEHP in adulthood exhibited increased *Acacb*, *Acss2*, and *Pdk4* hepatic mRNA expression (65).

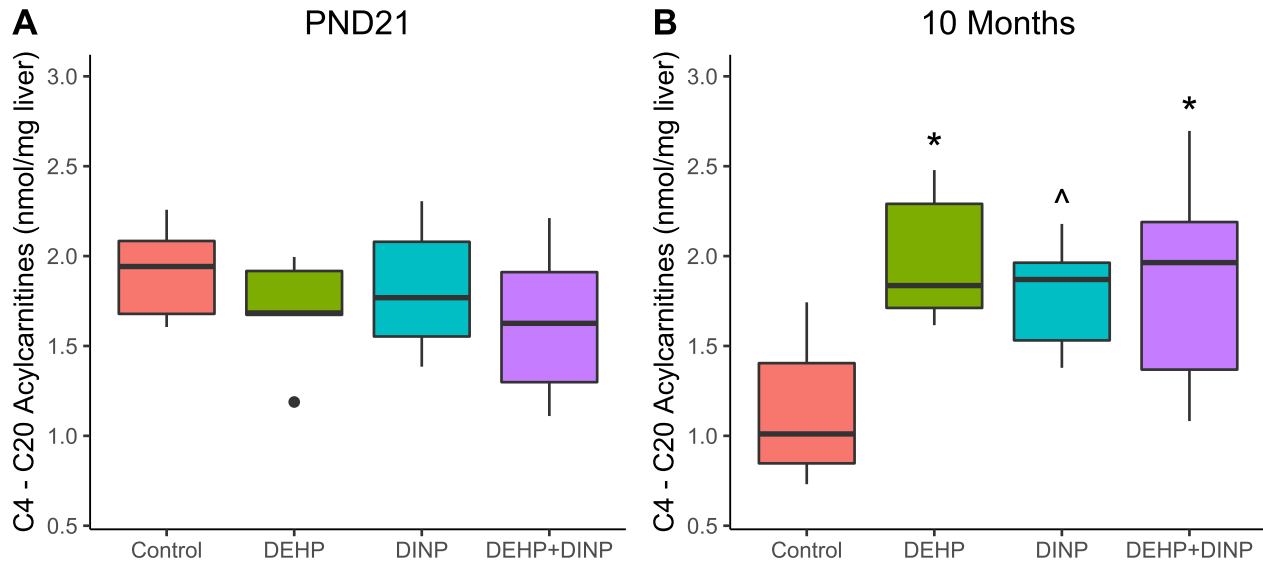


Figure 7: Differences in hepatic C4–C20 acylcarnitine levels between phthalate-exposed and control females. Log-transformed levels of even-numbered C4–C20 acylcarnitines across exposure groups in livers from females at (A) PND21 (N=6/group) and (B) 10 months of age (N=6/group). In boxplots, the boxes represent the IQR and lines extend to 1.5*IQR, while dots are observations outside 1.5*IQR. Comparisons of acylcarnitine levels between exposure groups and the control group were evaluated with multiple linear regression of log-transformed data with the control as the reference group. Corrections for multiple comparisons were made using a Bonferroni correction factor. ^P < 0.10, *P < 0.05 versus controls

		RNA-seq Differential Expression	Pathway Analysis	RNA-seq/ RT-qPCR	Bisulfite- Pyrosequencing	Targeted Metabolomics	
Objective		Unbiased screen for changes in gene expression	Utilize RNA-seq data to identify persistently altered biological pathways	Follow up analyses on candidate PPAR target genes driving acetyl-CoA metabolism pathway		Measurement of DNA methylation at CpG sites in the promoter near PPAR binding sites	Assess functional outcomes of metabolic gene pathway perturbation
				RNA-seq counts	RT-qPCR		
Results	DEHP: PND21	61 DE genes	0 enriched GOBP pathways; PPAR α and PPAR γ identified as TFs	Acly Cs Fasn	Acly Cs Fasn	Acly Cs Fasn \uparrow	Acetyl-CoA Acylcarnitines
	DEHP: 10 months			Acly Cs Fasn \uparrow	Acly Cs Fasn	Acly Cs Fasn	Acetyl-CoA Acylcarnitines \uparrow
	DINP: PND21	1 DE gene	13 enriched GOBP pathways; top pathway = acetyl-CoA metabolism; PPAR α and PPAR γ identified as TFs	Acly Cs Fasn \uparrow	Acly Cs Fasn \uparrow	Acly Cs Fasn \uparrow	Acetyl-CoA Acylcarnitines
	DINP: 10 months			Acly Cs Fasn \uparrow	Acly Cs Fasn \uparrow	Acly Cs Fasn \uparrow	Acetyl-CoA \uparrow Acylcarnitines \uparrow
	DEHP+DINP: PND21	1 DE gene	13 enriched GOBP pathways; top pathway = acute phase response; PPAR α and PPAR γ identified as TFs	Acly Cs Fasn \uparrow	Acly Cs Fasn \uparrow	Acly Cs Fasn \downarrow	Acetyl-CoA \downarrow Acylcarnitines
	DEHP+DINP: 10 months			Acly Cs Fasn	Acly Cs Fasn \uparrow	Acly Cs Fasn \downarrow	Acetyl-CoA \uparrow Acylcarnitines \uparrow
Summary		DINP females show most robust response in metabolic/PPAR target gene expression		DINP has persistent \uparrow gene expression; DEHP has \uparrow at 10 months; DEHP+DINP has \uparrow primarily at PND21	All groups show altered DNAm in promoter regions; only modest persistent change is Fasn in DINP; promoter Acly DNAm associated with expression at PND21	DEHP+DINP has \downarrow in acetyl-CoA at PND21 and \uparrow acetyl-CoA at 10 months. DINP has modest \uparrow in acetyl-CoA at 10 months. All groups have \uparrow or modest \uparrow in acylcarnitines at 10 months	

Figure 8: Summary of findings in females perinatally exposed to phthalates. Overall workflow of experiments and analyses are indicated at the top with orange arrows. Corresponding findings are depicted below. Solid blue up arrows indicate significantly increased versus controls (P < 0.05) and solid red arrows indicate significantly decreased versus controls (P < 0.05). Corresponding outlined arrows represent trends towards significance (P < 0.10). DE, differentially expressed; DNAm, DNA methylation; GOBP, gene ontology biological processes; TFs, transcription factors

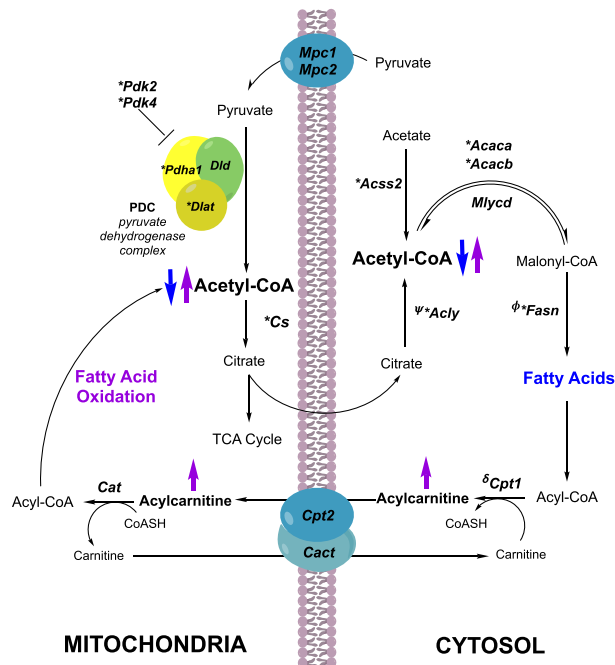


Figure 9: Metabolic pathways connecting gene expression, DNA methylation, and targeted metabolomic data. Arrows represent conversion of one metabolite to another and –| indicates negative regulation. Italicized genes encode enzymes responsible for these enzymatic conversions. *Denotes genes in the acetyl-CoA metabolic process pathway that were up-regulated in one or more phthalate-exposed groups of females relative to controls via edgeR QLF differential expression analyses at either PND21 or 10 months with unadjusted P-values <0.10. Decreased hepatic acetyl-CoA levels observed in phthalate-exposed females at PND21 (blue arrows) in conjunction with up-regulation of the genes outlined above suggest that acetyl-CoA was being used for production of fatty acids at PND21. Increased hepatic acetyl-CoA and acylcarnitine levels observed in 10-month females perinatally exposed to phthalates (purple arrows) in conjunction with up-regulation of the genes outlined above suggest that oxidation of fatty acids was increasing acetyl-CoA production. δ Cpt1b mRNA expression was increased in phthalate-exposed 10-month females via post hoc examination of RNA-seq edgeR QLF differential expression results, further supporting that fatty acid oxidation was increased. ψ Increased Acly mRNA expression as measured via RT-qPCR and decreased Acly promoter DNA methylation were associated with decreased acetyl-CoA levels at PND21, and increased ϕ Fasn promoter DNA methylation was associated with decreased acetyl-CoA levels at PND21

Furthermore, Ren *et al.* found that the effects of DEHP on hepatic gene expression of *Acacb*, *Acss2*, and *Pdk4* were PPAR α -dependent. Although we could not identify any studies that examined expression of *Cs* or *Dlat* in the liver following phthalate exposures, one study found that *Cs* and *Dlat* were up-regulated in the hearts of mice exposed to DEHP in adulthood (66), which is consistent with our data. *Fasn* mRNA expression was up-regulated in the livers of mice perinatally exposed to another environmental obesogen, tributyltin, as well as the PPAR γ agonist rosiglitazone (67), which was similar to our findings with respect to phthalates in the present study. However, direct exposure to DEHP in adulthood has been associated with decreased hepatic *Fasn* gene expression (68). Also in contrast to our findings, previous studies indicated that direct treatment of PPAR α and PPAR γ agonists to adult mice resulted in increased, not decreased, *Mlycd* expression in the liver (69, 70).

We found some evidence of persistent exposure-related changes in DNA methylation in the promoter regions of the PPAR target gene *Fasn*, but in general, promoter DNA methylation did not fully explain gene expression or hepatic metabolite levels. DNA methylation was persistently increased in the *Fasn*

promoter in DINP females at both PND21 and 10 months, although the magnitude of differences between DINP-exposed females and controls were smaller at 10 months. In addition, *Fasn* promoter region DNA methylation and expression were both increased with perinatal phthalate exposure, which was unanticipated based on the conventional views of the relationship between promoter methylation and gene expression. However, sequencing BSC DNA cannot distinguish between 5mC and 5hmC. Thus, this increase in DNA methylation may be explained by an increase in 5hmC. TET enzymes are recruited to target regions by PPARs, and increased promoter 5hmC levels have been associated with increased gene expression (26, 71). In addition, previous work in our lab found that developmental exposure to another EDC, bisphenol-A (BPA), influenced 5hmC levels longitudinally across the genome in mouse blood, especially in imprinted gene regions, demonstrating that developmental EDC exposures are capable of altering 5hmC (72).

Our data indicated sex-specific effects of developmental phthalate exposures on hepatic gene expression pathways. Since phthalates have been implicated in interfering with sex hormones (73), sexually dimorphic effects following phthalate exposures were expected. Females perinatally exposed to DINP exhibited the most prominent differential gene expression in the liver, and gene set enrichment analysis revealed different metabolic pathways impacted by developmental phthalate exposures in females and males. Furthermore, our previous studies indicated that females were more susceptible to long-term metabolic effects, including glucose intolerance and body fat accumulation, than males following perinatal phthalate exposures (34). In contrast, a previously published study examining liver reprogramming following developmental DEHP exposures found sex-specific reprogramming in males but not females; however, this study examined glycogen storage/depletion as the main outcome of interest, utilized higher doses of DEHP, analyzed younger mice, and only evaluated hepatic expression of one gene (74). Other researchers who examined hepatic gene expression in mice perinatally exposed to a mixture of food contaminants, including DEHP, observed increased gene expression of cholesterol-related genes in males only (75). However, this chemical mixture included other chemicals with diverse modes of action, including BPA, polychlorinated biphenyl 153, and 2,3,7,8-tetrachlorodibenzo-*p*-dioxin. Additional studies are needed to fully elucidate the underlying mechanisms driving sex-specific effects of developmental phthalate exposures on metabolic pathways in the liver.

A majority of previous studies that have examined metabolic impacts of developmental phthalate exposures have focused on investigating DEHP. The inclusion of DINP and a mixture of DEHP+DINP in the present study is unique and also of critical importance in the context of public health due to trends indicating that exposure to DEHP is declining while exposure to DINP is increasing in women of reproductive age in the US population (6). Furthermore, humans are exposed to mixtures of phthalates, and it is therefore important to understand metabolic impacts of developmental phthalate mixture exposures. Our findings with respect to DINP and a mixture of DEHP+DINP in the present study, combined with whole-body metabolic phenotyping data published in previous studies highlight the need for continued examination of this phthalate. Perinatal exposure to a mixture of DEHP+DINP was associated with changes in PPAR target gene expression, promoter methylation, acetyl-CoA levels, and acylcarnitine levels in female livers. Notably, our data indicated that females perinatally exposed to DEHP+DINP had increased hepatic expression of

some PPAR target genes at PND21, but in most cases, these effects did not persist to 10 months of age. Furthermore, alterations in hepatic acetyl-CoA and acylcarnitines were age-specific. This was consistent with our previous phenotyping studies that indicated females perinatally exposed to DEHP+DINP had increased body weight and relative liver weight at PND21, but did not exhibit these same phenotypes longitudinally (31, 34). Additional work is needed to fully understand these complex mixture effects.

The data presented in this study provide evidence that metabolic pathways, including PPAR-regulated target genes, were altered in the liver in mice perinatally exposed to phthalates in early postnatal life and in adulthood, long after exposure had ceased. However, our study was limited in multiple ways. The transcriptomics analysis included only six mice per group, which is a relatively small number and likely influenced the power to detect subtle differences in a perinatal exposure study such as this one. None of the PPAR target genes that we examined had an FDR < 0.10 when analyzing the entire transcriptome, and log fold changes (LFCs) in genes that had un-adjusted P-values of < 0.05 ranged from -0.45 to 2.49. In addition, our analyses were on bulk liver tissue, and we did not measure whether cellular composition of the liver was altered in phthalate-exposed mice. Therefore, we were unable to determine the extent to which perinatal phthalate exposures reprogrammed the cells of the liver, versus the cellular composition of the liver. In addition, although RT-qPCR data generally agreed with RNA-seq data, it did not for *Cs* and *Fasn* in 10-month livers. Importantly, our DNA methylation assays only covered between 3 and 10 CpG sites per assay, so there may be other CpGs within the promoter region or enhancer regions that have regulatory effects on gene transcription that we did not measure. Our findings indicated an association between DNA methylation in the *Acy* promoter and *Acy* gene expression at PND21, even with small effect sizes. However, we did not find similar associations between promoter methylation and gene expression for *Fasn* or *Cs*. It is possible that our assays did not capture the most relevant regulatory CpGs, or captured CpGs that when methylated or unmethylated result in a state 'poised' for gene expression, but not necessarily active gene expression (76). Future studies should consider methods that cover larger regions of the genome, such as reduced representation bisulfite sequencing or whole-genome bisulfite sequencing, to identify regions that are altered by perinatal phthalate exposures and play a role in regulating PPAR target gene expression. Finally, our transcriptomic, DNA methylation, and targeted metabolomic data indicate that in the liver of female mice perinatally exposed to phthalates, acetyl-CoA may be preferentially utilized for fatty acid synthesis at PND21 and fatty acid oxidation at 10 months, but we did not directly trace acetyl-CoA through different metabolites. Thus, it is possible that the altered levels of acetyl-CoA we observed were due to additional or other underlying mechanisms.

Conclusion

Overall, our data suggest that perinatal exposures to phthalates have both short- and long-term effects on liver metabolism in female mice, particularly on acetyl-CoA and fatty acid metabolism pathways, which are processes regulated by PPARs. In early postnatal life when mice were still directly exposed to phthalates, gene expression and metabolite patterns were suggestive of a shift in metabolism towards fatty acid biosynthesis. However, at 10 months of age, long after exposure ceased, liver metabolism appeared to have increased fatty acid oxidation.

Metabolic pathways were impacted by perinatal exposure to DINP, as well as a mixture of DEHP+DINP, demonstrating the need for increased animal and human studies evaluating metabolic effects of DINP and phthalate mixtures. Our data indicate that hepatic metabolic responses to perinatal phthalate exposures are different depending on age, suggesting that age and/or time since exposure play a role in metabolic effects of developmental phthalate exposures. This was consistent with previously published work that demonstrated age-specific increases in body weight and body fat in females perinatally exposed to phthalates, further demonstrating the ability of phthalates to interfere with metabolism. Additional studies are needed in other metabolic tissues such as skeletal muscle, cardiac muscle, and adipose tissue to determine whether similar PPAR target genes are impacted across multiple tissue types and to provide more context for how molecular mechanisms influence whole-body metabolic effects.

Acknowledgments

The authors would like to thank Anna Atkins with assistance in with managing samples for RNA-seq, as well as Bambarendage (Pinithi) Perera, Christine Rygiel, Leah D. Bedrosian, and Drew Cheatham for their assistance with tissue collections.

Supplementary data

Supplementary data are available at *EnvEpig* online.

Funding

This work was supported by the University of Michigan (UM) National Institute of Environmental Health Sciences (NIEHS)/Environmental Protection Agency (EPA) Children's Environmental Health and Disease Prevention Center P01 ES022844/RD83543601, and the Michigan Lifestage Environmental Exposures and Disease (M-LEEaD) NIEHS Core Center (P30 ES017885). Targeted metabolomic analyses were supported by the National Institute of Diabetes, Digestive, and Kidney Diseases (NIDDK) under award number P30DK089503 (MNORC). K.N. was supported by the UM NIEHS Institutional Training Grant T32 ES007062 and National Institute of Child Health and Human Development (NICHD) Institutional Training Grant T32 HD079342.

Conflict of interest statement. None declared.

References

1. Moore JX, Chaudhary N, Akinjemiju T. Metabolic syndrome prevalence by race/ethnicity and sex in the United States, National Health and Nutrition Examination Survey. *Prev Chronic Dis* 1988;14:2012.
2. Schettler T. Human exposure to phthalates via consumer products. *Int J Androl* 2006;29:134–9.
3. Buckley JP, Engel SM, Braun JM, Whyatt RM, Daniels JL, Mendez MA, Richardson DB, Xu Y, Calafat AM, Wolff MS, Lanphear BP, Herring AH, Rundle AG. Prenatal phthalate exposures and body mass index among 4- to 7-year-old children: a pooled analysis. *Epidemiology* 2016;27:449–58.
4. Buckley JP, Engel SM, Mendez MA, Richardson DB, Daniels JL, Calafat AM et al. Prenatal phthalate exposures and childhood

- fat mass in a New York City Cohort. *Environ Health Perspect* 2016;**124**: 507–13. Retrieved from <http://ehp.niehs.nih.gov/1509788>
5. Harley KG, Berger K, Rauch S, Kogut K, Claus Henn B, Calafat AM, Huen K, Eskenazi B, Holland N. Association of prenatal urinary phthalate metabolite concentrations and childhood BMI and obesity. *Pediatr Res* 2017;**82**:405–15.
 6. Carlson KR, Garland SE. Estimated phthalate exposure and risk to pregnant women and women of reproductive age as assessed using four NHANES biomonitoring data sets (2005/2006, 2007/2008, 2009/2010, 2011/2012). 2015.
 7. Lapinskas PJ, Brown S, Leesnitzer LM, Blanchard S, Swanson C, Cattley RC, Corton JC. Role of PPAR α in mediating the effects of phthalates and metabolites in the liver. *Toxicology* 2005;**207**:149–63.
 8. Sarath Josh MK, Pradeep S, Vijayalekshmi Amma KS, Balachandran S, Abdul Jaleel UC, Doble M, et al. Phthalates efficiently bind to human peroxisome proliferator activated receptor and retinoid X receptor α , β , γ subtypes: an in silico approach. *J Appl Toxicol* 2018;**34**:754–65. Available from: <http://www.ncbi.nlm.nih.gov/pubmed/23843199>.
 9. Kaya T, Mohr SC, Waxman DJ, Vajda S. Computational Screening of phthalate monoesters for binding to PPAR γ . *Chem Res Toxicol* 2006;**19**:999–1009.
 10. Valles EG, Laughter AR, Dunn CS, Cannelle S, Swanson CL, Cattley RC et al. Role of the peroxisome proliferator-activated receptor alpha in responses to diisononyl phthalate. *Toxicology* 2003;**191**:211–25.
 11. Bility MT, Thompson JT, McKee RH, David RM, Butala JH, Heuvel, VJP et al. Activation of mouse and human peroxisome proliferator-activated receptors (PPARs) by phthalate monoesters. *Toxicol Sci* 2004;**82**:170–82.
 12. Ehrenborg E, Krook A. Regulation of skeletal muscle physiology and metabolism by peroxisome proliferator-activated receptor. *Pharmacol Rev* 2009;**61**:373–93.
 13. Shao X, Wang M, Wei X, Deng S, Fu N, Peng Q et al. Peroxisome proliferator-activated receptor- γ : master regulator of adipogenesis and obesity. *Curr Stem Cell Res Ther* 2016;**11**:282–9.
 14. Wang Y-X, Lee C-H, Tiep S, Yu RT, Ham J, Kang H, Evans RM. Peroxisome-proliferator-activated receptor δ activates fat metabolism to prevent obesity. *Cell* 2003;**113**:159–70.
 15. Fan W, Evans R. PPARs and ERRs: molecular mediators of mitochondrial metabolism. *Curr Opin Cell Biol* 2015;**33**:49–54.
 16. Auboeuf D, Rieusset J, Fajas L, Vallier P, Frering V, Riou JP, Staels B, Auwerx J, Laville M, Vidal H. Tissue distribution and quantification of the expression of mRNAs of peroxisome proliferator-activated receptors and liver X receptor-alpha in humans: no alteration in adipose tissue of obese and NIDDM patients. *Diabetes* 1997;**46**:1319–27.
 17. Kliewer SA, Forman BM, Blumberg B, Ong ES, Borgmeyer U, Mangelsdorf DJ, Umesono K, Evans RM. Differential expression and activation of a family of murine peroxisome proliferator-activated receptors. *Proc Natl Acad Sci U S A* 1994;**91**:7355–9.
 18. Echeverría F, Ortiz M, Valenzuela R, Videla LA. Long-chain polyunsaturated fatty acids regulation of PPARs, signaling: relationship to tissue development and aging. *Prostaglandins Leukot Essent Fat Acids* 2016;**114**:28–34.
 19. Lendvai Á, Deutsch MJ, Plösch T, Ensenaer R. The peroxisome proliferator-activated receptors under epigenetic control in placental metabolism and fetal development. *Am J Physiol Metab* 2016;**310**:E797–810.
 20. Wang Y, Chen B, Lin T, Wu S, Wei G. Protective effects of vitamin E against reproductive toxicity induced by di(2-ethylhexyl) phthalate via PPAR-dependent mechanisms. *Toxicol Mech Methods* 2017;**27**:551–9.
 21. Hayashi Y, Ito Y, Yamagishi N, Yanagiba Y, Tamada H, Wang D, Ramdhan DH, Naito H, Harada Y, Kamijima M, Gonzales FJ, Nakajima T. Hepatic peroxisome proliferator-activated receptor α may have an important role in the toxic effects of di(2-ethylhexyl)phthalate on offspring of mice. *Toxicology* 2011;**289**:1–10.
 22. Fujiki K, Shinoda A, Kano F, Sato R, Shirahige K, Murata M. PPAR γ -induced PARylation promotes local DNA demethylation by production of 5-hydroxymethylcytosine. *Nat Commun* 2013;**4**:2262.
 23. Medvedeva YA, Khamis AM, Kulakovskiy IV, Ba-Alawi W, Bhuyan MSI, Kawaji H, Lassmann T, Harbers M, Forrest ARR, Bajic VB. Effects of cytosine methylation on transcription factor binding sites. *BMC Genomics* 2014;**15**:119.
 24. Ito S, Shen L, Dai Q, Wu SC, Collins LB, Swenberg JA, He C, Zhang Y. Tet proteins can convert 5-methylcytosine to 5-formylcytosine and 5-carboxylcytosine. *Science* (80-) 2011;**333**:1300–3.
 25. Sun F, Abreu-Rodriguez I, Ye S, Gay S, Distler O, Neidhart M, Karouzakis E. TET1 is an important transcriptional activator of TNF α expression in macrophages. Chen L, editor. *PLoS One* 2019;**14**:e0218551.
 26. Xu X, Tan X, Tampe B, Wilhelmi T, Hulshoff MS, Saito S, Moser T, Kalluri R, Hasenfuss G, Zeisberg EM, Zeisberg M. High-fidelity CRISPR/Cas9- based gene-specific hydroxymethylation rescues gene expression and attenuates renal fibrosis. *Nat Commun* 2018;**9**:3509.
 27. Reik W, Dean W, Walter J. Epigenetic reprogramming in mammalian development. *Science* 2001;**293**:1089.
 28. Smallwood SA, Kelsey G. De novo DNA methylation: a germ cell perspective. *Trends Genet* 2012;**28**:33–42.
 29. Zeng Y, Chen T. DNA Methylation reprogramming during mammalian development. *Genes (Basel)* 2019;**10**:257.
 30. Saitou M, Kagiwada S, Kurimoto K. Epigenetic reprogramming in mouse pre-implantation development and primordial germ cells. *Development* 2012;**139**:15–31.
 31. Neier K, Cheatham D, Bedrosian LD, Dolinoy DC. Perinatal exposures to phthalates and phthalate mixtures result in sex-specific effects on body weight, organ weights and intracisternal A-particle (IAP) DNA methylation in weanling mice. *J Dev Orig Health Dis* 2019;**10**:176–87. Retrieved from https://www.cambridge.org/core/product/identifier/S2040174418000430/type/journal_article
 32. Lee SS, Pineau T, Drago J, Lee EJ, Owens JW, Kroetz DL, Fernandez-Salguero PM, Westphal H, Gonzalez FJ. Targeted disruption of the alpha isoform of the peroxisome proliferator-activated receptor gene in mice results in abolishment of the pleiotropic effects of peroxisome proliferators. *Mol Cell Biol* 1995;**15**:3012–22.
 33. Palkar PS, Anderson CR, Ferry CH, Gonzalez FJ, Peters JM. Effect of prenatal peroxisome proliferator-activated receptor α (PPAR α) agonism on postnatal development. *Toxicology* 2010;**276**:79–84.
 34. Neier K, Cheatham D, Bedrosian LD, Gregg BE, Song PX, Dolinoy DC. Longitudinal metabolic impacts of perinatal exposure to phthalates and phthalate mixtures in mice. *Endocrinology* 2019;**160**:1613–30.
 35. Waterland RA, Jirtle RL. Transposable elements: targets for early nutritional effects on epigenetic gene regulation. *MCB* 2003;**23**:5293–300.

36. Weinhouse C, Anderson OS, Bergin IL, Vandenberg DJ, Gyekis JP, Dingman MA, et al. Dose-dependent incidence of hepatic tumors in adult mice following perinatal exposure to bisphenol A. *Environ Health Perspect* 2014;**122**:485–91. Retrieved from <http://ehp.niehs.nih.gov/1307449/>
37. Schmidt J-S, Schaedlich K, Fiandanese N, Pocar P, Fischer B. Effects of di(2-ethylhexyl) phthalate (DEHP) on female fertility and adipogenesis in C3H/N mice. *Environ Health Perspect* 2012;**120**:1123–9.
38. Lin Y, Wei J, Li Y, Chen J, Zhou Z, Song L, Wei Z, Lv Z, Chen X, Xia W, Xu S. Developmental exposure to di(2-ethylhexyl) phthalate impairs endocrine pancreas and leads to long-term adverse effects on glucose homeostasis in the rat. *Am J Physiol Metab* 2011;**301**:E527–38.
39. Hannas BR, Lambright CS, Furr J, Howdeshell KL, Wilson VS, Gray LE. Dose-response assessment of fetal testosterone production and gene expression levels in rat testes following in utero exposure to diethylhexyl phthalate, diisobutyl phthalate, diisooheptyl phthalate, and diisononyl phthalate. *Toxicol Sci* 2011;**123**:206–16.
40. Lorber M, Calafat AM. Dose reconstruction of di(2-ethylhexyl) phthalate using a simple pharmacokinetic model. *Environ Health Perspect* 2012;**120**:1705–10.
41. Wittassek M, Angerer J, Kolossa-Gehring M, Schäfer SD, Klockenbusch W, Dobler L, Günzel AK, Müller A, Wiesmüller GA. Fetal exposure to phthalates—a pilot study. *Int J Hyg Environ Health* 2009;**212**:492–8.
42. Wittassek M, Angerer J. Phthalates: metabolism and exposure. *Int J Androl* 2008;**31**:131–8.
43. Chang J-W, Lee C-C, Pan W-H, Chou W-C, Huang H-B, Chiang H-C, Huang P-C. Estimated daily intake and cumulative risk assessment of phthalates in the general taiwanese after the 2011 DEHP food scandal. *Sci Rep* 2017;**7**:22.
44. Silva MJ, Reidy JA, Herbert AR, Preau JL, Needham LL, Calafat AM. Detection of phthalate metabolites in human amniotic fluid. *Bull Environ Contam Toxicol* 2004;**72**:1226–31.
45. Huang P-C, Tsai C-H, Liang W-Y, Li S-S, Huang H-B, Kuo P-L. Early phthalates exposure in pregnant women is associated with alteration of thyroid hormones. Gonzalez-Bulnes A, editor. *PLoS One* 2016;**11**:e0159398.
46. Huang P, Kuo P, Chou Y, Lin S, Lee C. Association between prenatal exposure to phthalates and the health of newborns☆. *Environ Int* 2009;**35**:14–20.
47. Calafat AM, Brock JW, Silva MJ, Gray LE, Reidy JA, Barr DB, Needham LL. Urinary and amniotic fluid levels of phthalate monoesters in rats after the oral administration of di(2-ethylhexyl) phthalate and di-n-butyl phthalate. *Toxicology* 2006;**217**:22–30.
48. Martin M. Cutadapt removes adapter sequences from high-throughput sequencing reads. *EMBnet J* 2011;**17**:10.
49. Andrews S. FastQC a quality control tool for high throughput sequence data. Retrieved from <http://www.bioinformatics.babraham.ac.uk/projects/fastqc/> (29 September 2020, date last accessed).
50. Dobin A, Davis CA, Schlesinger F, Drenkow J, Zaleski C, Jha S, Batut P, Chaisson M, Gingeras TR. STAR: ultrafast universal RNA-seq aligner. *Bioinformatics* 2013;**29**:15–21.
51. Li B, Dewey CN. RSEM: accurate transcript quantification from RNA-seq data with or without a reference genome. *BMC Bioinformatics* 2011;**12**:323.
52. Robinson MD, McCarthy DJ, Smyth GK. edgeR: a Bioconductor package for differential expression analysis of digital gene expression data. *Bioinformatics* 2010;**26**:139–40.
53. McCarthy DJ, Chen Y, Smyth GK. Differential expression analysis of multifactor RNA-seq experiments with respect to biological variation. *Nucleic Acids Res* 2012;**40**:4288–97.
54. Love MI, Huber W, Anders S. Moderated estimation of fold change and dispersion for RNA-seq data with DESeq2. *Genome Biol* 2014;**15**:550.
55. Sartor MA, Leikauf GD, Medvedovic M. LRpath: a logistic regression approach for identifying enriched biological groups in gene expression data. *Bioinformatics* 2009;**25**:211–7.
56. Lee C, Patil S, Sartor MA. RNA-Enrich: a cut-off free functional enrichment testing method for RNA-seq with improved detection power. *Bioinformatics* 2016;**32**:1100–2.
57. Qin Q, Fan J, Zheng R, Wan C, Mei S, Wu Q, Sun H, Brown M, Zhang J, Meyer CA, Liu XS. LISA: inferring transcriptional regulators through integrative modeling of public chromatin accessibility and ChIP-seq data. *Genome Biol* 2020;**21**:32.
58. Mosteller F, Fisher RA. Questions and answers. *Am Stat* 1948;**2**:30.
59. Vandesompele J, De Preter K, Pattyn F, Poppe B, Van Roy N, De Paeppe A, Speleman F. Accurate normalization of real-time quantitative RT-PCR data by geometric averaging of multiple internal control genes. *Genome Biol* 2002;**3**:research0034.1.
60. Liu T, Ortiz JA, Taing L, Meyer CA, Lee B, Zhang Y, Shin H, Wong SS, Ma J, Lei Y, Pape UJ, Poidinger M, Chen Y, Yeung K, Brown M, Turpaz Y, Liu XS. *Genome Biol* 2011;**12**:R83.
61. Sas KM, Kayampilly P, Byun J, Nair V, Hinder LM, Hur J, Zhang H, Lin C, Qi NR, Michailidis G, Groop P-H, Nelson RG, Darshi M, Sharma K, Schelling JR, Sedor JR, Pop-Busui R, Weinberg JM, Soleimanpour SA, Abcouwer SF, Gardner TW, Burant CF, Feldman EL, Kretzler M, Brosius FC, Pennathur S. Tissue-specific metabolic reprogramming drives nutrient flux in diabetic complications. *JCI Insight* 2016;**1**:e86976.
62. Koves TR, Ussher JR, Noland RC, Slentz D, Mosedale M, Ilkayeva O, Bain J, Stevens R, Dyck JRB, Newgard CB, Lopaschuk GD, Muoio DM. Mitochondrial overload and incomplete fatty acid oxidation contribute to skeletal muscle insulin resistance. *Cell Metab* 2008;**7**:45–56.
63. Zhang Y. Likelihood-based and Bayesian methods for Tweedie compound Poisson linear mixed models. *Stat Comput* 2013;**23**:743–57.
64. Jakobsen JS, Waage J, Rapin N, Bisgaard HC, Larsen FS, Porse BT. Temporal mapping of CEBPA and CEBPB binding during liver regeneration reveals dynamic occupancy and specific regulatory codes for homeostatic and cell cycle gene batteries. *Genome Res* 2013;**23**:592–603.
65. Ren H, Aleksunes LM, Wood C, Vallanat B, George MH, Klaassen CD, Corton JC. Characterization of peroxisome proliferator-activated receptor α -independent effects of PPAR α activators in the rodent liver: di-(2-ethylhexyl) phthalate also activates the constitutive-activated receptor. *Toxicol Sci* 2010;**113**:45–59.
66. Li W, Zhang W, Chang M, Ren J, Zhuang X, Zhang Z, Cui Y, Chen H, Xu B, Song N, Li H, Shen G. Quadrupole orbitrap mass spectrometer-based metabolomic elucidation of influences of short-term di(2-ethylhexyl) phthalate exposure on cardiac metabolism in male mice. *Chem Res Toxicol* 2018;**31**:1185–94.
67. Chamorro-García R, Sahu M, Abbey RJ, Laude J, Pham N, Blumberg B. Transgenerational inheritance of increased fat depot size, stem cell reprogramming, and hepatic steatosis elicited by prenatal exposure to the obesogen tributyltin in mice. *Environ Health Perspect*. 2013;**121**: 359–66. Retrieved from <http://ehp.niehs.nih.gov/1205701>

68. Eveillard A, Lasserre F, de Tayrac M, Polizzi A, Claus S, Canlet C, Mselli-Lakhal L, Gotardi G, Paris A, Guillou H. Identification of potential mechanisms of toxicity after di-(2-ethylhexyl)-phthalate (DEHP) adult exposure in the liver using a systems biology approach. *Toxicol Appl Pharmacol* 2009;**236**:282–92.
69. Lee GY, Kim NH, Zhao Z-S, Cha BS, Kim YS. Peroxisomal-proliferator-activated receptor alpha activates transcription of the rat hepatic malonyl-CoA decarboxylase gene: a key regulation of malonyl-CoA level. *Biochem J* 2004;**378**:983–90.
70. Rogue A, Renaud MP, Claude N, Guillouzo A, Spire C. Comparative gene expression profiles induced by PPAR γ and PPAR α/γ agonists in rat hepatocytes. *Toxicol Appl Pharmacol* 2011;**254**:18–31.
71. Wu H, D'Alessio AC, Ito S, Wang Z, Cui K, Zhao K, Sun YE, Zhang Y. Genome-wide analysis of 5-hydroxymethylcytosine distribution reveals its dual function in transcriptional regulation in mouse embryonic stem cells. *Genes Dev* 2011;**25**:679–84.
72. Kochmanski JJ, Marchlewicz EH, Cavalcante RG, Perera BPU, Sartor MA, Dolinoy DC. Longitudinal effects of developmental bisphenol A exposure on epigenome-wide DNA hydroxymethylation at imprinted loci in mouse blood. *Environ Health Perspect* 2018;**126**:077006.
73. Mylchreest E, Wallace DG, Cattley RC, Foster PM. Dose-dependent alterations in androgen-regulated male reproductive development in rats exposed to di(*n*-butyl) phthalate during late gestation. *Toxicol Sci* 2000;**55**:143–51.
74. Maranghi F, Lorenzetti S, Tassinari R, Moracci G, Tassinari V, Marcoccia D, Di Virgilio A, Eusepi A, Romeo A, Magrelli A, Salvatore M, Tosto F, Viganotti M, Antoccia A, Di Masi A, Azzalin G, Tanzarella C, Macino G, Taruscio D, Mantovani A. In utero exposure to di-(2-ethylhexyl) phthalate affects liver morphology and metabolism in post-natal CD-1 mice. *Reprod Toxicol* 2010;**29**:427–32.
75. Naville D, Pinteaur C, Vega N, Menade Y, Vigier M, Le Bourdais A, Labaronne E, Debard C, Luquain-Costaz C, Bégeot M, Vidal H, Le Magueresse-Battistoni B. Low-dose food contaminants trigger sex-specific, hepatic metabolic changes in the progeny of obese mice. *FASEB J* 2013;**27**:3860–70.
76. Matsumura Y, Nakaki R, Inagaki T, Yoshida A, Kano Y, Kimura H, Tanaka T, Tsutsumi S, Nakao M, Doi T, Fukami K, Osborne TF, Kodama T, Aburatani H, Sakai J. H3K4/H3K9me3 bivalent chromatin domains targeted by lineage-specific DNA methylation pauses adipocyte differentiation. *Mol Cell* 2015;**60**:584–96.